The Dissertation Committee for Mansoureh Peydayesh
certifies that this is the approved version of the following dissertation:

Using Fast-Responding Resources to Control Frequency in a Power System

Committee:

Ross Baldick, Supervisor

Surya Santoso

Aristotle Arapostathis

James Eric Bickel

Parviz Adib

Using Fast-Responding Resources to Control Frequency in a Power System

by

Mansoureh Peydayesh, BSEE; MSEE

DISSERTATION

Presented to the Faculty of the Graduate School of

The University of Texas at Austin

in Partial Fulfillment

of the Requirements

for the Degree of

DOCTOR OF PHILOSOPHY

THE UNIVERSITY OF TEXAS AT AUSTIN

December 2016

To Him,

who is with me in all moments!

To my husband and son,

who stand behind me in all steps.

To my mother and father,

who spend their lives building mine.

To my only sister and brother-in-law,

who are the kindest and the dearest.

Acknowledgments

First, foremost and solely, I thank God, the most merciful, the all-knowing and the almighty, for everything.

I wish to extend my gratitude to my supervisor Dr. Ross Baldick for his advice and support throughout my PhD. Dr. Baldick supported me intellectually and financially. I have learned a lot from his vast knowledge and insightful questions. I am privileged to have had the opportunity to work with him.

I would like to extend my appreciation to my committee members, Dr. Surya Santoso, Dr. Aristotle Arapostathis, Dr. Eric Bickel, and Dr. Parviz Adib for their time and valuable comments.

I would like to sincerely thank Dr. Julia Matevosyan for all her invaluable help and support during and even after my internship at the Electric Reliability Council of Texas (ERCOT). Also, I would like to thank all my colleagues in ERCOT especially Karthik Gopinath, Sreenivas Badri, Joel Koepke, Sandip Sharma, Pengwei Du, Kenneth Ragsdale, and Fred Huang for all their kind help, fruitful discussions, and valuable comments.

I appreciate the time I spent and the discussions I had with my colleagues in Energy System Laboratory at the University of Texas at Austin, especially Dr. Mahdi Kefayati and Mohammad Majidi. I also thank Ms.

Melanie Gulick, the graduate coordinator of the Electrical and Computer Engineering department.

I would like to express my most sincere gratitude to my beloved husband for supporting me in every aspects of life. I would also like to mention my precious son who was born in the middle of my PhD and lighted our life. I am greatly thankful to both of them for being so patient and helpful throughout my journey as a PhD student.

I should never forget the continuous energy and love I got from my mom and dad. May God endow them with the best of rewards and compensate all their hard efforts to be such perfect parents. Finally, I thank my sister and her husband especially for filling my empty space in the family during these years.

Using Fast-Responding Resources to Control Frequency in a Power System

Publication No. _____

Mansoureh Peydayesh, Ph.D.
The University of Texas at Austin, 2016

Supervisor: Ross Baldick

Frequency control is one of the major concerns of power system operators. Frequency varies as the result of a supply-demand mismatch. Due to possible destructive outcomes of large frequency variations, several mechanisms are in operation to keep supply and demand in balance. Increasing penetration of non-dispatchable intermittent generation resources may increase power supply volatility, which makes frequency control more challenging.

Emerging utility-scale storage technologies with reasonable cost have participated in electricity markets in recent years. Because of fast-ramping capabilities of these resources, one of their attractive applications is providing frequency regulation service. However, the amount of energy they can produce or consume is limited due to their restricted storage capabilities. Thus, in spite of their fast response to a deployment signal, their duration of response is bounded.

In this thesis, we focus on using fast-responding resources to control frequency in power systems. In this research, the first question is if the participation of these resources in the regulation market have any adverse effect on the frequency control performance of the system. If the answer is yes, the next question is what is the best strategy to not only prevent the negative consequences but also improve the benefits of using fast-responding resources for frequency control.

For this research, the system of Electric Reliability Council of Texas (ERCOT) is selected. All power system studies related to frequency control require an appropriate dynamic model. In this dissertation, a simplified model is constructed, which represents the ERCOT system frequency response during a short period of time after a contingency. The model is validated and tuned against system frequency measured by Phasor Measurement Units. Especially in situations of not having information about system individual units, this simplified model is highly advantageous. However, to study system frequency during normal conditions, a more comprehensive model is essential. Thus, we develop ERCOT Frequency Modeling and Analysis Tool (EFMAT), which has the required level of details and accuracy to simulate system frequency. All proposed approaches of modeling and parameter tuning in this research are also applicable to other power systems.

In order to answer our research questions, we start with investigation of ERCOT Fast-Responding Regulation Service (FRRS). For selected historic days, conventional regulation providers are replaced by a storage system pro-

viding FRRS. For various capacities of the storage system, frequency is simulated using EFMAT and a system frequency control performance index is calculated. Comparing calculated index of different simulations can reveal the effect of FRRS capacity on the system performance.

The simulations are repeated for several FRRS deployment strategies similar to the strategies of other North America power markets along with our proposed modifications. Three different storage systems are assumed in the simulations: one with unlimited stored energy, one with 6 minutes energy duration, and one with 15 minutes energy duration.

Finally, FRRS optimal capacity and equivalency ratio between FRRS and conventional regulation are defined and calculated for the best deployment strategy.

Table of Contents

List of Tables

List of Figures

Chapter 1

Introduction

1.1 Outline

This chapter serves as an introduction to this dissertation and is organized in three sections. Section 1.2 will present a literature background on the modeling of power system for frequency control studies. Section 1.3 will introduce the concept of providing frequency regulation by fast-responding resources and explore the relevant literature. Finally, Section 1.4 will provide an overview of the dissertation.

1.2 Modeling Power System for Frequency Control Studies

One of the essential tasks in a power system is to keep frequency within the required range around the system nominal frequency. A large frequency deviation from its nominal value could have undesirable consequences such as damaging equipment, degrading load performance, causing the transmission lines to be overloaded, interfering with system protection schemes, and eventually leading to an unstable condition in the power system [6]. Special control schemes, pre-defined actions, and operational limitations during both normal and emergency conditions are required to satisfy the frequency obligations of

a power system.

Frequency response of a power system is the system's reaction to a contingency (such as loss of a generation unit) in order to restore frequency to the nominal value [20, 22]. Various aspects of power system management from real-time operation to long-term planning usually involve system frequency response assessment for which a proper dynamic model of the power system is essential. Such a model is also required for other studies regarding frequency control such as adjusting frequency relays, estimation of required spinning reserve, and limitation of non-dispatchable generators.

One approach to construct a dynamic model for a power system is to include all generation units, load resources, and the transmission system and obtain model parameters through various tests. This kind of model is usually used by the industry to study the dynamic performance of power systems, evaluate future system potential, and set up system operating limits [21, 25, 48]. However, needed information and required operational data to construct this model may not be public or accessible for all researchers. On the other hand, these complicated models may not be required for all studies.

Another approach to model a power system is to develop a simple equivalent model. Typically, these models calculate the average frequency behavior of the system [2] by ignoring synchronizing oscillations between generators and assuming a uniform frequency value throughout the system. An example of this approach is a system frequency response (SFR) model developed to estimate the response of a power system to sudden load or generation disturbances

in [2]. This model assumes that most of generating units in the power system are reheat steam turbine units. Therefore, all units are represented by a single equivalent reheat steam turbine unit with a simplified dynamic model. Reference [2] suggested that the values of equivalent unit parameters normalized on the total system base will be the same as values of a single unit parameters normalized on the unit base. This model has been used in several studies to predict frequency deviation and design an Under Frequency Load Shedding (UFLS) scheme [3, 10, 52, 68, 71, 72, 78]. However, this model cannot properly characterize a power system having different types of generating units other than reheat steam turbine. For such a system, another study [1] replaced all units from each dominant generation type with one equivalent unit. Although all those equivalent units are represented with the reheat steam turbine model used in [2], the units have different values for their parameters.

Each generation type has its own dynamic model. Modeling all generation types by steam turbine model and different parameter values may not fully represent dynamic behavior of various types. Having separate models for dominant generation types will be more valuable if each type is represented by its own dynamic model.

The performance of a model depends on having both proper structure and accurate parameters. To practically determine the values of parameters, it is necessary to have a clear and straightforward method that is applicable to a general power system. Using typical unit parameters for the simplified model of the system is recommended in [2] and is adopted by many researchers.

However, defining typical parameters for actual power systems may not be practical nowadays because different units of a system of varying vintages have been manufactured by different manufacturers and with different parameter values.

In recent decades, data from Phasor Measurement Units (PMUs) provides the opportunity to validate and calibrate system components' models [28, 30, 39, 62] and system-wide models [11, 12, 29].

Frequency control in a power system is necessary not only in a short period of time after each contingency event but also continuously during system normal operation. This continuous control is usually accomplished by means of regulation service. Next section will introduce frequency regulation service provided by fast-responding resources.

1.3 Utilizing Fast-Responding Resources to Control Frequency

Frequency deviation from nominal value is a consequence of an imbalance between power production by generators and power consumption by loads in a power system. Short-term frequency control especially during system normal operation is the responsibility of load frequency control (LFC) system. In restructured electricity markets, this type of frequency control is usually categorized as an ancillary service called regulation. Thermal generators, which have traditionally provided regulation service, change their output in response to the LFC signal in order to compensate for the power imbalance and thus,

lower frequency deviation.

In recent years, the penetration of intermittent non-dispatchable resources, such as wind turbines and photovoltaic (PV) units, has increased. Rapid and uncertain changes in the outputs of these resources may lead to faster frequency dynamics which result in fast-changing LFC signal. Responding to a fast-changing LFC signal will decrease operational efficiency of thermal generators and cause extra wear and tear which will increase maintanance cost [63]. In addition, thermal generators may not be able to perfectly track fast-changing LFC signal due to their limited ramp rates [13].

Energy storage systems convert electricity to another form of energy (such as mechanical or chemical) and store it for use at a later time. In the past, storage systems (besides pumped-storage hydro) were not widely used in power systems because of their limited capacity and high cost. However, in recent years, emerging technologies with acceptable capacity and cost have become available for use in power systems. High efficiency, rapid response, and better ramping capability of energy storage systems make them attractive resources to provide regulation service. However, the amount of stored energy in these fast-responding resources is limited, which may cause their failure in providing continuous regulation service. In fact, using these technologies in order to control frequency is a trade-off between fast response and limited duration of response. Hence, a combination of thermal generators and fast-responding resources is preferable for regulation provision in most power systems.

Some studies have shown that storage can be more effective than con-

ventional generators in providing regulation service [46, 49, 50, 73], meaning that a MW of storage systems is not equivalent to a MW of conventional generators in frequency regulation. A study by the Pacific Northwest National Laboratory (PNNL) defines an "ideal" fast-responding resource as one with "instantaneous response, perfect accuracy, and unlimited energy" [49]. This study proposes a "peak shaving approach", which deploys regulation service whenever area control error (ACE) goes beyond a defined dead zone. PNNL observes that if regulation is provided by a combustion turbine, the required procured capacity to perfectly control ACE would be equal to 2.7 times the required procured capacity when regulation is provided by the defined ideal resource.

Despite the energy limitations of storage systems, these technologies could provide more effective regulation compared to combustion turbines, steam turbines, or combined-cycle turbines [46]. Another study prepared for the California Energy Commission (CEC) further supports these claims, concluding that on an incremental basis, storage can be up to two to three times as effective as adding a combustion turbine to the system for regulation purposes [50]. This means that a 100 MW energy storage system can be as effective as 200-300 MW of combustion turbine capacity dedicated to providing regulation [46]. Also, the Federal Energy Regulatory Commission (FERC) Order Number 755 [17] observes that if faster-ramping resources replace conventional resources in providing regulation, Regional Transmission Organizations (RTOs) and Independent System Operators (ISOs) may procure less regulation capac-

ity. Furthermore, faster ramping could result in a more accurate response to the LFC signal and avoid overshooting. However, the traditional regulation payment method was solely based on the capacity reserved for regulation and did not acknowledge the greater amount of frequency regulation service being provided by faster-ramping resources. Consequently, FERC required all RTOs and ISOs in its jurisdiction to have a two-level compensation format based on both capacity and performance of regulation providers [17].

Capability of fast-responding resources is not the only factor in using them as frequency regulation providers. Several studies have considered the optimal sizing of these resources [7, 13, 51, 63]. The regulation capacities of thermal generators and storage are optimized in [63] based on the proposed regulation allocation method with the goal of minimizing the overall regulation cost. A general procedure is presented in [51] to find optimal size and optimal operation of a storage system by maximizing its operating profit. Also, offer strategies are proposed in [26, 27, 76] in order to maximize the economic benefits of fast-responding resources by maximizing their participation in regulation market. On the other hand, some studies explore issues related to fast-responding resources providing regulation with the purpose of improving power system frequency control performance instead of economic objectives [13, 37, 64].

One important issue in all of these studies is how to dispatch fast-responding resources and what signal they should follow to provide regulation service. Historic LFC signals from different markets were used in [7, 36, 43, 49,

63, 76] to show the benefits of regulation service provided by fast-responding resources and also, represent the effectiveness of proposed strategies to better utilize these resources. However, provision of a significant amount of regulation by these resources will cause changes in the frequency from its historic value, which will result in a LFC signal different from the historic LFC signal. Thus, it is not logical to use historic signals to prove the effectiveness of fast-responding regulation service. Investigating the effects of this service needs a proper model of a power system that represents the closed loop performance. Simple closed loop models are used in some studies [13, 51] but the models do not include detailed aspects of a real power system affecting frequency dynamics.

Performance of faster-ramping resources is not the only factor in their level of effectiveness in providing frequency control. Other important factors are system policies on how to use these resources. New frequency regulation policies have been implemented by some power system operators in order to facilitate the participation of fast-responding resources in regulation markets [74]. One of these new policies is to design control strategies which specify how to dispatch these resources. If these strategies do not provide enough opportunity for fast-responding resources to help frequency control, they may even deteriorate system frequency control performance. A necessary tool to investigate this issue is a proper system model including all different types of frequency control and considering all system features and market policies which may affect frequency.

1.4 Overview of the Dissertation

The first step of any frequency control study is to select a proper model. As discussed in Section 1.2, previously proposed models need improvements.

In this dissertation, frequency response of the system of Electric Reliability Council of Texas (ERCOT) is modeled based on dynamic models of dominant generation types. The proposed model is validated and tuned using PMU data. The underlying approach of modeling and parameter tuning is applicable to other power systems.

As explained before, a system frequency response model simulates the frequency behavior of the system just after a contingency event and is not sufficient for frequency analysis in non-emergency conditions. Studies related to frequency control during system normal operation require a proper system model including different types of frequency control and considering system features and market policies which may affect frequency. Hence, ERCOT Frequency Modeling and Analysis Tool (EFMAT) is developed in this dissertation which is able to simulate frequency over a time horizon up to 24 hours. The method of developing this tool is also applicable to other power systems.

A subset of regulation service in ERCOT is fast responding regulation service (FRRS) provided by resources with almost unlimited ramp rates in response to a specifically designed signal [59]. The effectiveness of FRRS service is studied in this dissertation and possible enhancements are investigated. In fact, the underlying goals of this research is to:

- verify if fast-responding resources can have any adverse effect,
- determine the issues to be considered in order to prevent unfavorable consequences, and
- explore strategies to improve the benefits of using fast-responding resources for frequency control.

The rest of this dissertation is organized as follows: Chapter 2 will discuss different frequency control mechanisms in a power system. Based on relevant mechanisms, a simplified model of frequency response of the ERCOT system will be constructed, validated, and tuned using PMU data in Chapter 3. In Chapter 4, ERCOT Frequency Modeling and Analysis Tool (EFMAT) will be introduced in details, verified and validated using historic operational data. Then, ERCOT fast-responding regulation service (FRRS) will be described and its effectiveness will be evaluated in Chapter 5. Other FRRS deployment logics will be examined in Chapter 6. Finally, Chapter 7 will conclude the dissertation and present future work.

Chapter 2

Power System Frequency Control

2.1 Introduction

A mismatch between mechanical power production and electricity consumption results in frequency deviation from its nominal value. Thus, keeping supply and demand in balance is essential to control frequency and requires accurate prediction of load. Despite the effort to forecast demand, there are second-by-second and minute-by-minute unpredictable variations in load, which result in differences between load and dispatched generation [9]. Also, increasing penetration of wind and other intermittent renewable resources will increase supply volatility that may lead to larger differences between load and generation. These differences will cause the frequency to fluctuate from its nominal value.

A power system has different levels of both inherent and designed frequency control schemes. Understanding these levels of control is the first step for studying and modeling power system frequency behavior. In the rest of this chapter, inertial frequency response and primary, secondary, and tertiary frequency controls will be explained.

2.2 Inertial Frequency Response

Any mismatch between supply and demand is a mismatch between mechanical torque and electromagnetic torque summed across all synchronous generators in the system. This mismatch results in changes in frequency of each generator. This reaction is called Inertial Frequency Response and is described by [40]:

$$\Delta P_m(t) - \Delta P_e(t) = 2H\frac{d\Delta f(t)}{dt} \tag{2.1}$$

where:

ΔP_m = mechanical power change (pu)
ΔP_e = electrical power change (pu)
H = inertia constant (MW.s/MVA)
Δf = frequency deviation from nominal (pu)

An additional issue is that frequency deviation affects the rotating speed of motor loads and as a result, their power consumption will change. Therefore, a portion of power system demand will vary due to frequency changes. Ignoring motor dynamics, this characteristic of electrical demand can be expressed by [40]:

$$\Delta P_e(t) = \Delta P_L(t) + D\Delta f(t) \tag{2.2}$$

where:

ΔP_e = electrical power change (pu)

ΔP_L = non-frequency-sensitive load change (pu)

$D\Delta f$ = frequency-sensitive load change (pu)

D = load-damping constant

Therefore, any change in load or generation is initially compensated by addition or extraction of kinetic energy from the rotating mass of synchronous generators and motors and consequently, the frequency will vary. Typical models used to study system frequency behavior are based on the idea of calculating the average frequency of the system [2]. The average frequency can be calculated by ignoring synchronizing oscillations between generators and assuming a uniform frequency value all through the system. Hence, all generators are represented by an equivalent generator with an equivalent inertia constant (H), which is driven by the sum of mechanical outputs of all turbines. Analogously, all system loads are replaced by a single load with an equivalent load-damping constant (D). Therefore, combining (2.1) and (2.2) will result in (2.3) which is called the Swing Equation and used to model the equivalent power system [40]:

$$\Delta P_m(t) - \Delta P_L(t) = 2H\frac{d\Delta f(t)}{dt} + D\Delta f(t) \tag{2.3}$$

where:

ΔP_m = total mechanical power change (pu)

ΔP_L = total non-frequency-sensitive load change (pu)

H = equivalent inertia constant (MW.s/MVA)

Δf = frequency deviation from nominal (pu)

D = equivalent load-damping constant

2.3 Primary Frequency Control

Beyond the natural inertial response of the system, each turbine is equipped with a governor, which senses frequency changes and modulates turbine input energy in order to limit the frequency excursion. This local automatic frequency control is usually referred as primary frequency control. However, primary frequency control can also be provided through the action of under-frequency relays that interrupt preset loads after frequency falls to a specified value.

Based on the North American Electric Reliability Corporation (NERC) standard, all units with capacity greater than 10 MW must have a governor in service. As frequency changes, the turbine governor modulates the main control valves to adjust the flow of working fluid through the turbine and accordingly, regulate the turbine mechanical power output.

Any governor has two characteristics: droop and deadband. Governor droop is the frequency drop, expressed as a percentage of nominal system frequency, causing governor to make 100% change in the unit's steady-state output. Governor deadband is a range of frequency deviation that will not activate the governor. Deadband was really a natural feature of the earliest governors caused by their physical characteristics. Intentional deadbands,

which are usually bigger than the physical ones, are used to reduce the governor activity during normal conditions of power system.

2.4 Secondary Frequency Control

Inertial frequency response and primary frequency control are decentralized and only able to limit and stop frequency excursions but are not well-suited to bring the frequency back to its target value. Instead, secondary frequency control is a centralized automatic control with the purpose of restoring the frequency to its scheduled value by controlling the output of selected units. As the deadband of secondary frequency control is usually smaller than a governor deadband, secondary control also maintains the generation-load balance when the governors are inactive.

The main objectives of secondary control, also called load frequency control (LFC), are maintaining frequency and controlling the net power interchanges with neighboring balancing authority areas at the scheduled values. In order to meet these objectives, a control error signal, called the area control error (ACE), is calculated. ACE is a linear combination of net interchange and frequency deviations and includes a frequency bias term, which requires each balancing area to increase generation when system frequency is low and decrease generation when frequency is high. The bias is specified in units of MW/0.1 Hz and is based on the MW size of the balancing area. After measuring and filtering the ACE, it is used as an input for a controller, which is usually a proportional integral (PI) controller. Based on the characteristics

of each control area, the resulting output signal is conditioned by limiters, delays, and gain constants. Then, the resulting control signal will be shared among units that are pre-selected to provide secondary control and sent to the units by means of the automatic generation control (AGC) system. Secondary control is typically provided just by a limited number of generation resources and not necessarily by all of them. [6, 38]

2.5 Tertiary Frequency Control

Tertiary control refers to actions taken to restore primary and secondary control reserves to manage current and future contingencies. This type of frequency control is slower than the other ones discussed earlier. Some examples of tertiary control are changing the base points of units, adjusting scheduled interchange, and connecting new generation units after a contingency [20, 47]. This type of control is usually achieved through Unit Commitment and Economic Dispatch after contingencies.

Chapter 3

Simplified Model of ERCOT Frequency Response

3.1 Introduction

Due to the importance of frequency control in a power system, the system performance in controlling frequency should be routinely evaluated and studies should be done on how to improve the system capability to keep the frequency nearly constant. On the other hand, any changes in a power system could affect the system frequency fluctuations. These effects should be studied before applying those changes in the system. All these studies usually need an accurate and simple model of the power system.

As defined previously, frequency response of a power system is the system's reaction to a contingency (such as loss of a generation unit) in order to restore frequency to the nominal value [20, 22] [1]. Several simplified models of system frequency response have been proposed previously [1, 2]. However, those models may not be appropriate and practical for all power systems as discussed in Section 1.2.

In this chapter, a simplified frequency response model is developed

[1] There might be more general definitions in other studies.

for the system of the Electric Reliability Council of Texas (ERCOT) which provides the electricity demand of 24 million consumers and about 90% of the total electricity demand of Texas. The ERCOT grid covers about 75% of the Texas land area with about 46,500 miles of transmission lines and more than 550 generation units having the total effective capacity of more than 77,000 MW to meet peak demand of approximately 71,000 MW [60, 61].

Frequency response of a power system is in fact frequency behavior during 10-15 seconds after a contingency. In this period of time, system frequency is mostly affected by inertial response of synchronous machines and primary frequency control from governors which will be modeled in the rest of this chapter in Section 3.2 and Section 3.3, respectively. As secondary and tertiary controls are slower than the other control types, their effects are negligible in this study time period. Hence, they are not included in the model.

Section 3.4 will describe dynamic models of ERCOT system dominant generation types. Section 3.5 will present the final model and Section 3.6 will explain model validation and tuning process.

3.2 Inertial Response Model

Similar to typical simplified models, a uniform frequency through the system is assumed in this model. So, all synchronous generators are represented by an equivalent generator driven by the sum of mechanical outputs of all turbines. Also, all load resources are replaced by a single load. The

equivalent system is modeled by the swing equation:

$$P_m(t) - P_l(t)(1 + D\Delta f(t)) = 2(H.MVA)\frac{d\Delta f(t)}{dt} \tag{3.1}$$

where:

P_m = total mechanical power (MW)

P_l = total load (MW)

D = equivalent load-damping constant

Δf = frequency deviation from nominal (pu)

$H.MVA$ = equivalent system inertia (MW.s)

This equation is slightly different from typical swing equation, as presented in Section 2.2, which is usually written in per unit of total system MVA. As a result, instead of H, this equation has $H.MVA$ term which is in fact equal to $\Sigma H_i.MVA_i$ summed over all synchronous generators, where H_i is the inertia constant of unit i in MW.s/MVA and MVA_i is the unit MVA capacity. Also, D is equivalent load-damping constant showing the total effect of frequency deviation on the frequency-sensitive loads.

Prior to a contingency event, mechanical power (P_m) and load (P_l) in the system are almost equal. When a contingency happens, mechanical power drops by the MW output of the lost generator (P_{Lost}). Then, due to the resulting frequency drop, governor systems adjust online units' mechanical power. In ERCOT, the primary frequency response is generally delivered completely within 12 to 14 seconds [69]. During this time period, load can be assumed

unchanged except for the part that is frequency-sensitive. Consequently, (3.1) can be re-written as:

$$-P_{Lost} + (\Delta P_m)(t) = 2(H.MVA)\frac{d\Delta f(t)}{dt} + DP_l\Delta f(t) \tag{3.2}$$

where ΔP_m is the change in total mechanical power of online units after contingency and is mostly due to governor control which will be modeled in next section.

3.3 Governor Model

At any time, droop and deadband of a governor determine required change in turbine output based on system frequency. Historically, most governors had steps in their output at the boundary of the deadband. From 2011, all units in ERCOT removed the step[2]. Governor request with and without step are shown in Figure 3.1. When frequency is out of deadband, governor request without step, which is used in our model, is calculated as:

$$P_{Gov} = -P_{Cap} * (\Delta f \pm (DB/60))/(R - (DB/60)) \tag{3.3}$$

where:

P_{Gov} = governor request (MW)

P_{Cap} = unit capacity (MW)

Δf = frequency deviation from nominal (pu)

[2]Personal communication with Sandip Sharma, Manager Operations Planning at ERCOT.

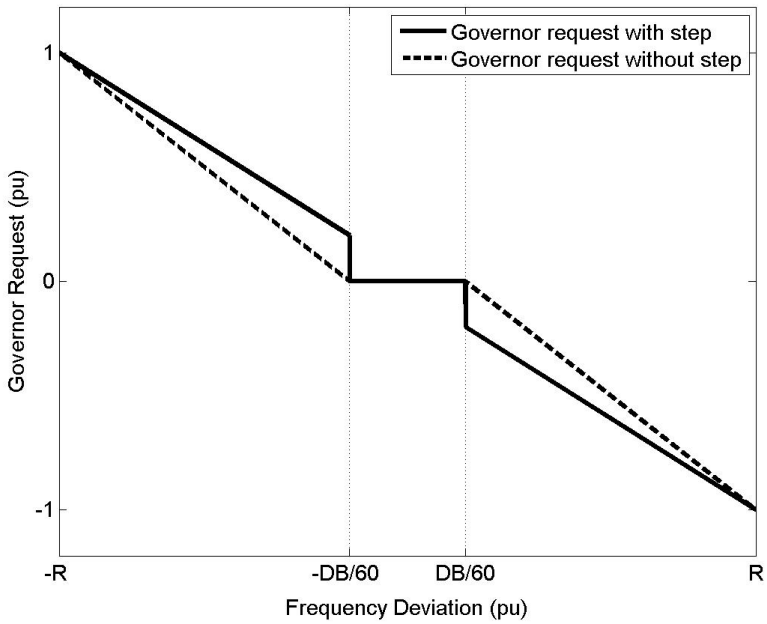

Figure 3.1: Governor request with/without step

DB = governor deadband (Hz)

R = governor droop

Unit's governor response, when frequency is below nominal frequency, is limited to headroom, i.e. the difference between unit high sustainable limit (HSL) and its current output. When frequency is above nominal frequency, unit's governor response is limited to legroom, i.e. the difference between units low sustainable limit (LSL) and its current output. Also, unit response to governor request is determined by the unit's dynamic characteristics, which will be discussed in the next section.

3.4 Dominant Generation Types

Governor request is in fact a control signal for the turbine. In our proposed model, dominant turbine types in the system should be determined in order to specify turbine responses to their governor requests. Then, all turbines of the same dominant type will be substituted by a single turbine, similar to the idea of [1]. However, in our model, each equivalent turbine is modeled based on the dynamic behavior of its own type. Any non-dominant turbine will be categorized with a dominant type having the greatest similarity in dynamic behavior.

Figure 3.2 shows the installed capacity of different generation technologies in ERCOT and its different zones in 2014 [23]. As will be discussed in this section, the steam unit dynamic model that is used in this study only consists of the model of steam turbine and does not contain the fuel system and steam production system. Therefore, all steam units can be represented by a single model regardless of their fuel type. That is, from the modeling perspective, coal fueled steam units, gas fueled steam units, and hydro units are all categorized as steam turbines. Although nuclear units should also be in the steam turbine group, they are not counted in this study as they do not provide governor response in ERCOT. In Figure 3.2, there is another category named "Peakers" which are generally combustion turbine units (commonly named single cycle gas turbine units) with two different types of fuel: oil or natural gas. As will be discussed in this section, single cycle gas turbine (SCGT) and combined cycle gas turbine (CCGT) units are categorized as gas turbines and

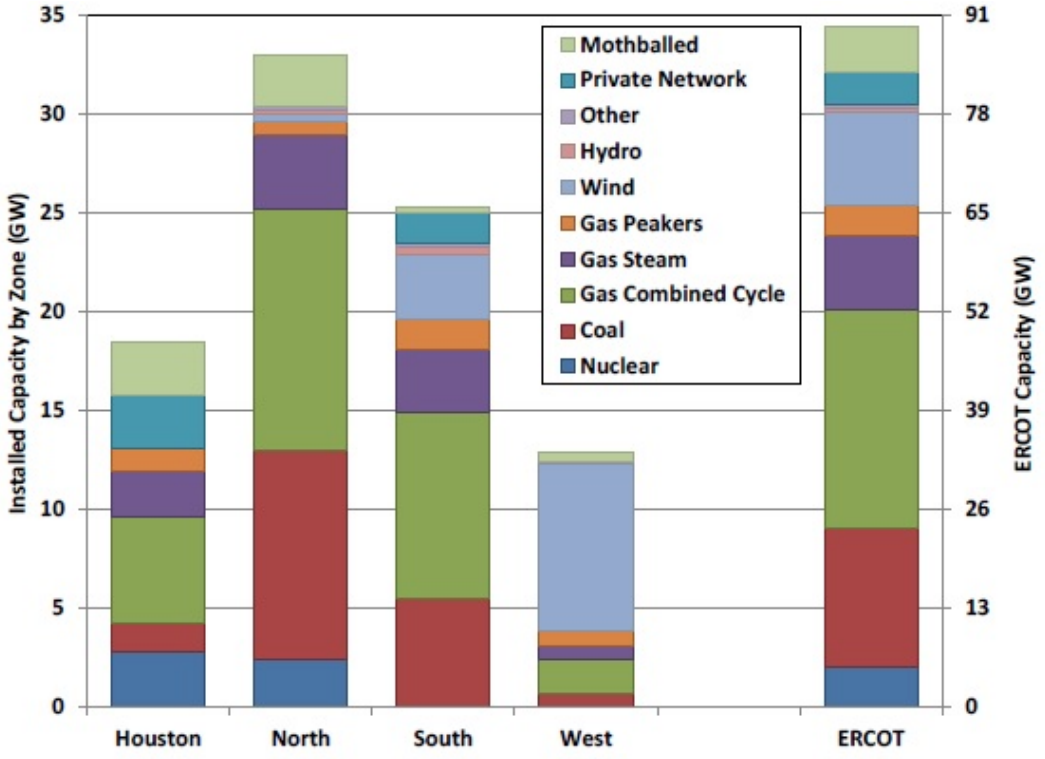

Figure 3.2: Installed capacity by technology in ERCOT (Source: Figure 54 of [23].)

represented by a single gas turbine unit.

In summary, based on Figure 3.2 and from the modeling perspective of this study, the dominant types of generation units in ERCOT are steam turbine, gas turbine, and wind turbine having approximately 44%, 37% and 13% respectively of the total installed capacity in year 2014.

After determining the dominant generation types, an appropriate model should be chosen for the equivalent unit of each type. Each power plant has

a high-order and detailed model developed by the plant manufacturer. This high-order model is capable of precisely representing the plant behavior under frequency changes. However, tuning this model needs burdensome data, and utilizing such a model for simulations poses computational difficulties [31]. Hence, several studies have created low-order models by simplifying high-order models while maintaining enough accuracy and precision for power system analysis. These low-order models are accurate enough for use in many power system analysis studies in place of detailed models [47].

The rest of this section will present a proper dynamic model for each dominant generation type of the ERCOT system.

3.4.1 Steam Turbine Model

In a steam-turbine power plant, a furnace fired by fossil fuels (coal, oil or gas) or a nuclear reactor (in nuclear units) provides heat for a boiler that produces steam. The stored energy of high-pressure and high-temperature steam will be transformed into mechanical rotating energy in the steam turbine. The steam turbine drives a generator, which finally converts mechanical energy into electricity. There are different strategies to control boiler and turbine operations. However, due to the slow dynamics of the boiler, its steam pressure could be assumed constant for a short period of time (around 10 seconds) [47, 65]. Therefore, to model the unit behavior right after a contingency in the system, it is valid to decouple boiler and turbine control. In other words, just the model of turbine is enough and the boiler model is not needed.

Figure 3.3 shows a simplified model of a steam turbine suitable for this study and constructed based on models proposed in [2, 40, 47, 65]. Governor block implements (3.3) and both turbine and governor dynamics are modeled with a single time constant (T_s).

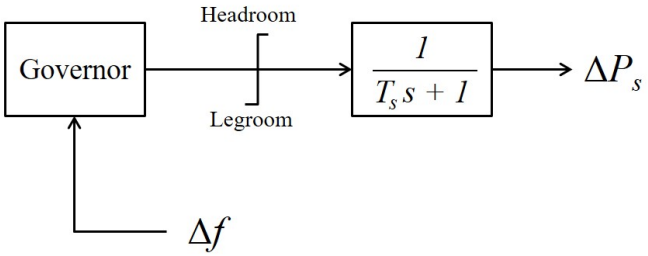

Figure 3.3: Steam turbine model

3.4.2 Gas Turbine Model

In a single cycle gas turbine (SCGT) power plant, the governor valve and the compressor supply fuel and compressed air to the combustion system. In the combustion system, the mixture of fuel and air is ignited and produces high-pressure and high-temperature combustion gas which is then directed into the gas turbine causing its rotation. If the power plant is a combined cycle gas turbine (CCGT) plant, the exhaust gas from the gas turbine is then directed into a heat recovery boiler. The produced steam finally rotates a steam turbine and generates more electricity. Most gas turbines used in power systems are heavy-duty single-shaft gas turbines that have all their masses (the compressor, combustor and turbine) mounted on the same shaft.

Several gas turbine models suitable for dynamic studies have been de-

veloped over the years. An excellent overview and comparative analysis of these models are given in [75]. A mathematical representation of a heavy-duty single-shaft gas turbine presented in [66] and [67] and became one of the most commonly used models. Several simplifications can be made to reduce the complexity of this model. However, the level of simplifications depends on the size and characteristics of the connected power system [66]. The gas turbine model is properly simplified for the purpose of this study in the rest of this section. All discussed details are mainly based on [4, 41, 42, 66, 67, 70, 75, 77].

The control system of a gas turbine has four control loops: acceleration control, speed control, temperature control, and airflow control. These control loops will be discussed in the following paragraphs.

Acceleration control is designed to prevent over-speeding of the generator and is usually used during unit start-up or in the unlikely event of a sudden separation from the power system. Therefore, the acceleration control loop can be omitted in our study.

The speed control system regulates the fuel supply based on unit base point and also system frequency by means of governor action which is of interest in this study. If the speed control system rapidly increases the fuel flow as a result of a system frequency drop, the exhaust temperature of the gas turbine may exceed its maximum allowable level imposed by turbine blade materials. Therefore, the temperature control system will override the speed control and lower the fuel signal until the temperature comes back to a safe level. In fact, the fuel signal is the output of a low value selector that has inputs from speed

control and temperature control.

Air flow control is done by modulating the inlet guide vane (IGV) that would only be in operation during start-up and shut-down of a SCGT. However, in a CCGT operating at partial load, IGV adjusts the air flow to optimize unit efficiency by keeping the exhaust temperature as high as possible. Hence, the airflow control is mainly affected by exhaust gas temperature.

If a gas turbine is connected to a relatively stiff system, where the frequency variations are not greater than $\pm 1\%$, the temperature control will not be activated except under a unit load lost event [66]. Thus, the temperature control and consequently, the air flow control can be ignored. ERCOT is a relatively stiff system as frequency drops are usually less than 1% (which is equal to 0.6 Hz). Even if frequency goes beyond 59.3 Hz (which is equal to 0.7 Hz or 1.17% drop), the first level of under-frequency load shedding will be activated and shed the load by 5% [56]. Therefore, it will be reasonable to eliminate the temperature and air flow control loops in our proposed model of a gas turbine. This might not be appropriate in a system with wider frequency variations.

Another important feature of a single-shaft gas turbine is its frequency dependency, which must be taken into account to make the model suitable for frequency control studies. Fuel control system works in such a way that the fuel flow rate is proportional not only to the fuel signal but also to the system frequency [66]. In a unit with liquid fuel, this frequency dependency is due to the fuel pumps driven at a speed proportional to the system frequency. How-

ever, this dependency in a unit with gas fuel is caused by the special design of different valves in the fuel control system. In addition, torque produced by the turbine has to be multiplied by frequency to calculate the mechanical power output of the turbine. Also, because of the turbine characteristics, produced torque depends both on the fuel flow and pressure ratio across the turbine which is a function of frequency. Thus, large frequency deviations, as in a generation trip event, affect the produced mechanical power of the turbine. This effect should be added to governor response in order to correctly calculate the changes in mechanical power compared to pre-contingency condition. Function f_1 discussed in Appendix A, calculates the frequency effect on the unit's output.

In a CCGT, the steam turbine produces typically approximately one third of the total power output [41]. Due to slow dynamics of the heat recovery boiler, the effect of gas turbine output change on the steam turbine output can be neglected. Also, the steam turbine component usually operates in sliding pressure mode and so does not provide governor response. Therefore, it is not needed to include the steam turbine components of a CCGT in our model. That will result in using the same model for both SCGT and CCGT units. However, it should be considered in the model that the capacity of the gas turbine in a CCGT unit is only around two thirds of CCGT total capacity. Thus, the capacity of equivalent gas turbine is equal to sum of SCGT units' capacity plus sum of two thirds of CCGT units' capacity. The same consideration should be done for turbine's headroom and legroom.

Figure 3.4 shows a model of gas turbine unit constructed based on gas turbine characteristics and all assumptions discussed above. Governor block implements (3.3) and both governor and turbine dynamics are modeled with a single time constant (T_g).

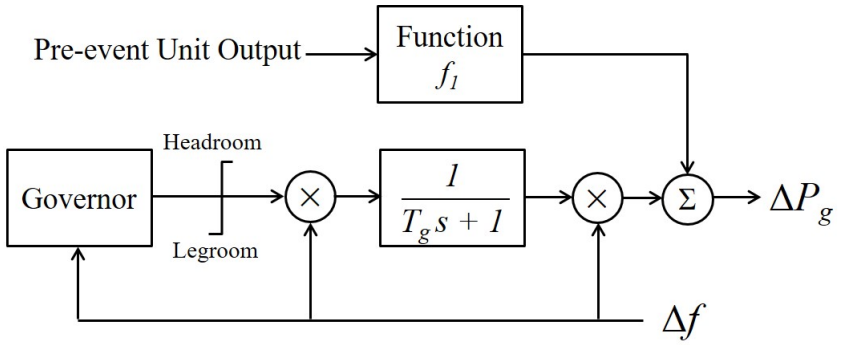

Figure 3.4: Gas turbine model

3.4.3 Wind Turbine Model

The output of a wind unit is usually equal to its HSL unless it was curtailed due to transmission constraints or power balance constraint. Therefore, most of the time wind units provide governor response only for over-frequency situations. They have governor response capability in under-frequency conditions when they are curtailed. In this study, the event of a generation unit trip is of interest, causing frequency drop. It is also assumed that there is no wind curtailment at the time of contingencies and as a result, no governor response from wind turbines. Therefore, wind turbines can be modeled as negative loads, and "Net Load" will be defined as load minus wind production.

3.5 Final ERCOT Model

Figure 3.5 shows the final model of the ERCOT system in which all turbines with a dominant type is replaced with a single turbine. In this model, equivalent steam turbine modeled as Figure 3.3 with capacity, headroom, and legroom equal to sum of capacity, headroom, and legroom of all committed steam turbines except nuclear units which do not provide governor response in ERCOT. Also, equivalent gas turbine modeled as Figure 3.4 with capacity, headroom, and legroom equal to sum of committed gas turbines' capacity, headroom, and legroom. It is assumed that gas turbine components in a CCGT have two thirds of total capacity, headroom, and legroom.

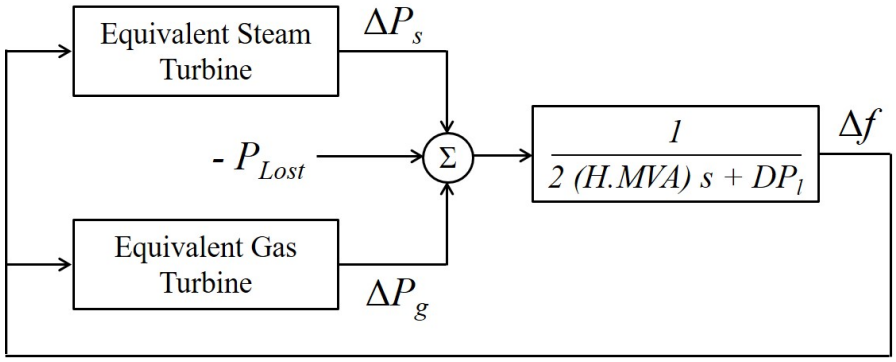

Figure 3.5: Final model of the ERCOT system

3.6 ERCOT Model Validation and Tuning

In power systems, phasor measurement units (PMUs) have several applications in different areas of system monitoring, protection, and control [12]. In early stages of installing PMUs in power systems, PMUs' data was found

to be beneficial for validating and calibrating different models used in power system simulations.

ERCOT has a large number of installed PMUs (more than 70 in 2014). In this study, frequency data measured by PMUs after 24 generating unit trip contingencies are utilized to calculate the unknown parameters of the ERCOT frequency response model constructed in previous sections. Due to oscillations between generators in the system, PMUs in different geographical locations may measure different frequencies. To remove these oscillations, at any time, the average of measured frequencies by all synchronized PMUs is calculated. Then, by using Simulink Design Optimization^{TM} tool, the model is fitted to data for the first 15 seconds after each event and the parameters are tuned. It should be mentioned that a model with a single steam turbine (similar to proposed model of reference [2]) may also be fitted to measured frequency after some contingencies. Even if the steam-only model manages to provide a good fit for the particular conditions studied, it is unlikely to provide a model that is good for other conditions. Also, tuned parameters will not have physical significance.

In order to tune our proposed model parameters, lost generation, system total load, wind production, capacities and pre-event outputs of the equivalent steam and gas turbines should be known for each contingency.

Traditionally, governor deadbands were set at 36 mHz which was the maximum limit based on NERC policy. During 2010-2012, governor deadbands of a few units in ERCOT were changed to 16.66 mHz. Since April 2014,

a NERC approved standard from Texas Reliability Entity has required generating units to set their governor deadbands not greater than 17 mHz except for those units with mechanical governors, which are required to have maximum deadband of 34 mHz [24]. The implementation plan of this standard allowed units to become compliant with these requirements before October 2015. As a result, all units changed their governor settings gradually during these 18 months. In order to assume 36 mHz governor deadbands for the equivalent turbines in the model, contingencies were selected from December 2011 till August 2014 during which time most of units in the system still had the old governor settings. The parameters calculation can be repeated in the future assuming 17 mHz deadbands based on events happening after 2016 when all units are compliant with new requirements.

Before implementation of this new standard, ERCOT units were required to set their governor droops not greater than $R = 5\%$ [56] which was initially selected for the proposed model. However, 5% droop was not consistent with empirical data for some of the events. To model this, droop was also included as a parameter to be determined from the empirical data, and its value was also tuned. This produced much better fits and meaningful values for other parameters.

As an example, Figure 3.6 shows the actual data for a contingency event that happened on December 30, 2011 along with best fits to the first 15 seconds of data, one with 5% droop assumption and the other with modeled droop parameter. It can easily be seen that the data was not consistent with

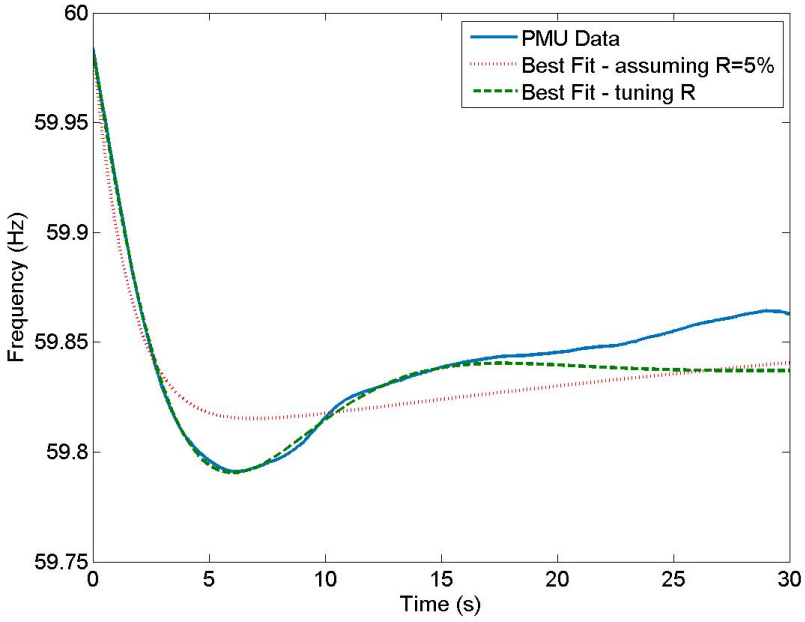

Figure 3.6: Actual measured frequency and the best fits of the model to the first 15 seconds of data after onset of an event on December 30, 2011

a 5% droop, which is nevertheless the "typical" value of droop for individual units. Also, the estimated value for steam turbine time constant in the fit assuming 5% droop was 130 seconds, which is not physically reasonable. It should be added that frequency rise in empirical data after 15 seconds is due to secondary frequency control which is not included in the proposed model. The simulated frequency is expected to stay constant after 20-25 seconds, which is also not satisfied in the fit assuming 5% droop. In summary, results showed that the droop parameter should be tuned.

Another model parameter is load damping constant. For 1 Hz change in frequency, ERCOT load changes by 1.5% during winter and 2.44% for the

rest of the year[3]. However, frequency change in the swing equation (3.1) used in this model is in per unit of nominal frequency instead of Hz. Therefore, equivalent load damping constant in (3.1) is equal to 60 multiplied by percent change in load due to 1 Hz change in frequency, which results in equivalent load damping constant equal to 0.9 during winter and 1.464 for the rest of the year.

Other unknown parameters that have to be calculated are the system inertia ($H.MVA$), the steam turbine time constant (T_s), and the gas turbine time constant (T_g). In the rest of this section, estimated values of unknown parameters for all events will be presented.

3.6.1 System Inertia

System inertia represents total mass of all synchronized generators in the system at the time of each contingency. As a rule of thumb, meeting more net load needs more generation resources to be committed which leads to larger system inertia. However, for the same level of net load, unit commitment may be different depending on predicted wind production, units' offer, time of day (peak hours, morning load pick-up, or evening load drop-off), and many other conditions. That is why for almost the same level of net load or even the same level of total thermal HSL, calculated values of system inertia based on contingency data can be different as shown in Figure 3.7 and Figure 3.8. However, fitting of empirical data produces a good estimate of system inertia

[3]Personal communication with Julia Matevosyan, Lead Planning Engineer at ERCOT.

based on net load or total thermal HSL. This estimation can be used in model simulation for future studies.

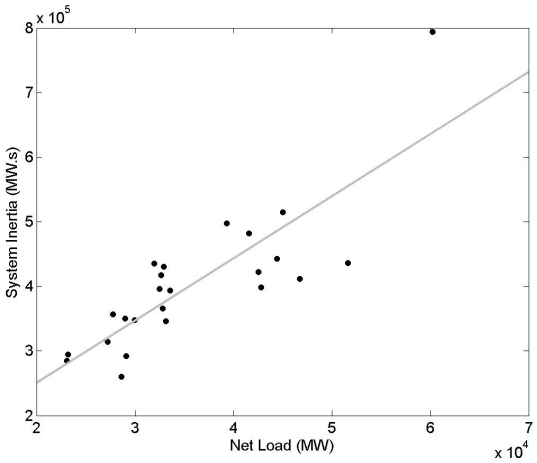

Figure 3.7: System inertia calculated for different contingencies vs. net load

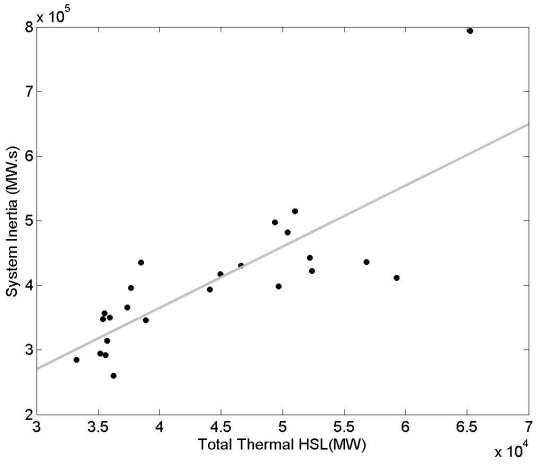

Figure 3.8: System inertia calculated for different contingencies vs. total thermal HSL

3.6.2 Governor Droop

In the model, governor droops of both equivalent gas and steam turbines are assumed equal. As discussed before, even if almost all of the units in the system have 5% governor droops, the model cannot be validated assuming 5% droop for equivalent units. This is mostly due to governor response being limited to available headroom of each unit which produces nonlinearities. Therefore, equivalent model with 5% droop even with limiting the governor response to total available headroom is not able to properly represent the system behavior.

The model droop is tuned against events' data. Figure 3.9 to Figure 3.11 show calculated droops versus net load, total thermal headroom, and total thermal HSL, respectively. A specific relation between calculated droop and other system conditions has not been found in this study. However, the calculated droops provide a range of tuned values to be used in model simulations that is better than using 5% droop.

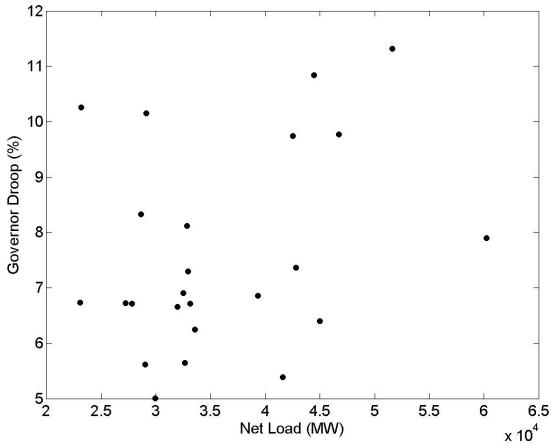

Figure 3.9: Governor droop calculated for different contingencies vs. net load

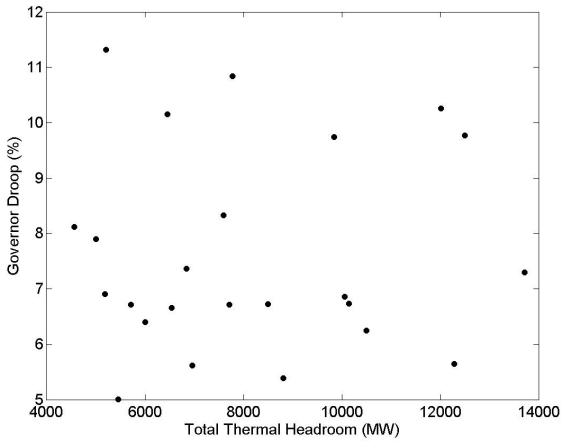

Figure 3.10: Governor droop calculated for different contingencies vs. total thermal headroom

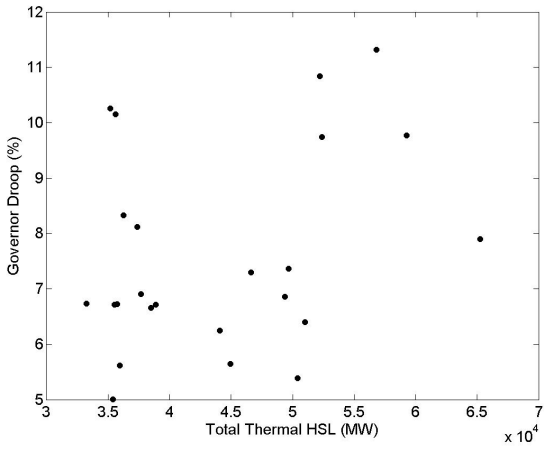

Figure 3.11: Governor droop calculated for different contingencies vs. total thermal HSL

3.6.3 Time Constants of Turbines

Last parameters to be estimated are the equivalent turbines' time constants. Figure 3.12 to Figure 3.15 show time constants versus HSLs and headrooms of equivalent turbines. Similar to governor droop, no specific relation has been found between time constants and other system conditions. However, tuned values of these two parameters are totally different from typical values of 0.2-0.5 seconds for an individual steam turbine [65] and 0.1-0.3 second for an individual gas turbine [67], which questions the validity of using typical parameter values for equivalent turbine models as recommended and adopted in some studies.

It is worth mentioning that variability of tuned time constants may be due to different committed units with different technologies and manufacturers. Also, output and other conditions of each system unit at the time of event may affect the modeled time constants.

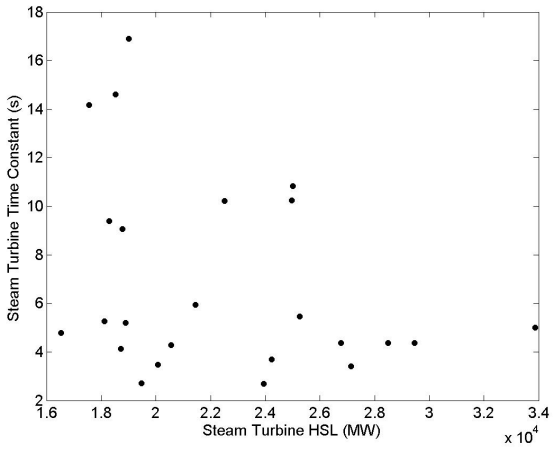

Figure 3.12: Steam turbine time constant calculated for different contingencies vs. steam HSL

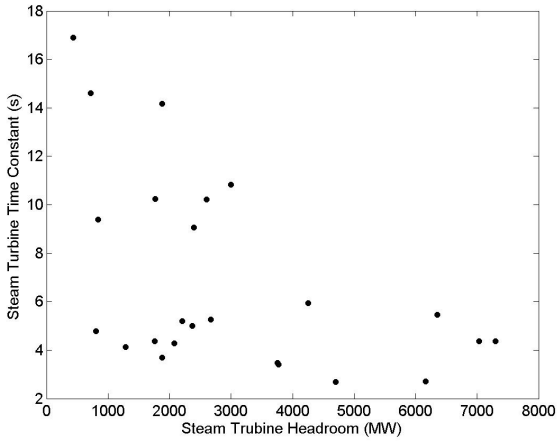

Figure 3.13: Steam turbine time constant calculated for different contingencies vs. steam headroom

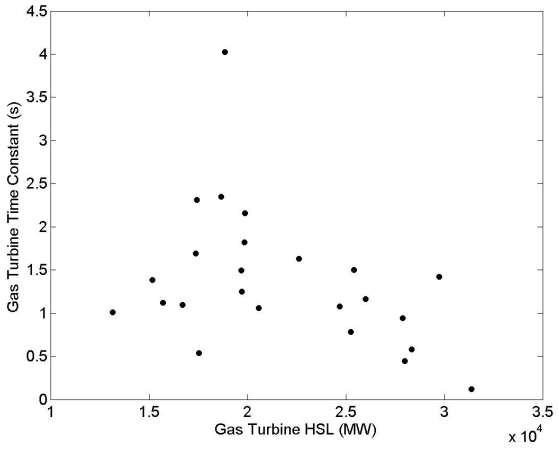

Figure 3.14: Gas turbine time constant calculated for different contingencies vs. gas HSL

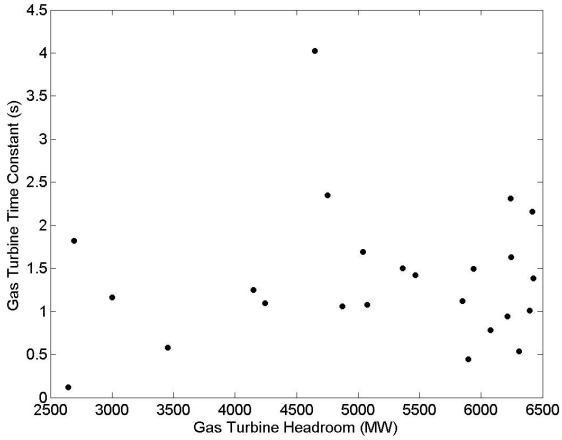

Figure 3.15: Gas turbine time constant calculated for different contingencies vs. gas headroom

Chapter 4

ERCOT Frequency Modeling and Analysis Tool

4.1 Introduction

The model discussed in Chapter 3 represents the ERCOT system frequency response (SFR) during a short period of time after a contingency. This simplified model is required and suitable for system studies such as predicting frequency nadir, adjusting under frequency relays, and estimation of required spinning reserve or system inertia to provide desirable frequency control. The proposed SFR model is also advantageous when there is the lack of information on system individual units and thus, the only solution is to have a few equivalent single units instead.

Studies on system frequency behavior during normal conditions need a more comprehensive dynamic model with adequate details of different frequency control levels and also processes affecting system frequency. As the ultimate goal of this dissertation is to investigate the effects of using fast-responding resources to provide regulation service, such a dynamic model is essential.

One solution is to extend the ERCOT SFR model of Chapter 3 to

include system frequency control levels other than inertial frequency response and primary frequency control, which are already included. However, without having information on individual units, it may not be practical to tune the unknown parameters of the extended model by using operational data.

Another solution is to add individual units' information without making the model intricate. Based on this idea, we developed ERCOT Frequency Modeling and Analysis Tool (EFMAT) which has the required level of details and accuracy to simulate system frequency. The main idea in this tool is to use system settings and measured data from a historic day. Based on the objective of each study, any aspects of the system can stay unchanged from historic values or can be altered as needed. Analyzing simulated frequency will reveal the effects of modified aspects on frequency control performance of the power system.

This tool relies on Excel and MATLAB^{TM}/Simulink^{TM}, and consists of three parts: pre-processing, Simulink model, and post-processing.

In the rest of this chapter, three different parts of EFMAT will be introduced in details in sections 4.2, 4.3, and 4.4. Then, several verification and validation tests done to authenticate EFMAT will be described in Section 4.5.

4.2 EFMAT Pre-Processing

First step for using EFMAT is to select a historic day to be modeled and gather all required data for that day. Pre-processing part includes two

macro-enabled Excel workbooks that obtain raw data and transform it to appropriate MATLAB variable format. This part also contains a list of all ERCOT units with their names, resource types, inertia constants, MVA basis, governor deadbands and droops, and also ratio of gas turbine capacity to total capacity for each combined cycle unit.

4.3 EFMAT Simulink Model

The second part is a model built in Simulink based on all different levels of frequency control in the ERCOT system.

Similar to typical frequency models, synchronizing oscillations between generators are ignored, frequency is assumed identical all over the system, and average system frequency is calculated based on the swing equation.

In this model, all generators in the system are replaced by a single equivalent generator driven by total mechanical power produced by all turbines. As wind units, photovoltaic units, and fast-responding resources (such as storage systems) do not provide inertial response, they are modeled separately. The power output of a storage system is assumed positive when it generates power (i.e. discharges) and negative when it consumes power (i.e. charges).

ERCOT is connected to other interconnections via direct power transmission lines (called "DC-ties"). Total energy flow of these ties is also considered in the model with positive sign for export and negative sign for import.

Considering all these aspects, the swing equation is re-written for the normal operation of the ERCOT system as:

$$P_{mech} + P_{wind} + P_{PV} + P_{FRR} - P_{ties} - P_{load}(1 + D\Delta f) = 2\,H.MVA\,\frac{d\Delta f}{dt} \quad (4.1)$$

where:

P_{mech} = total mechanical power produced by thermal generators (MW)

P_{wind} = total generation of wind units (MW)

P_{PV} = total generation of photovoltaic units (MW)

P_{FRR} = total output of fast-responding resources (MW)

P_{ties} = total DC ties' flow (MW)

P_{load} = system load (MW)

D = equivalent load-damping constant

Δf = frequency deviation from nominal (pu)

$H.MVA$ = total system inertia (MW.s/MVA)

The final goal of this dissertation is to study fast-responding regulation service. Hence, in simulations, different features of this service have to be varied from historic settings which will change total output of fast-responding resources (P_{FRR}). As a result, simulated frequency will be different from historic frequency. This is an important issue to be considered in order to decide what aspects of the system can stay unchanged from historic values and what aspects have to be calculated during simulations. This issue is also relevant to any other frequency study.

In (4.1), total generation of wind units (P_{wind}), total generation of PV units (P_{PV}), total flow of DC ties (P_{ties}), and system load (P_{load}) are independent of system frequency and can stay unchanged from historic values. However, two facts should also be considered. First, ERCOT requires primary response from wind turbines. Thus, total governor response from wind units has to be calculated during a simulation based on simulated frequency and added to historic wind production. Second, historic measured load ($P_{measured\ load}$) was slightly affected by historic frequency variations. Therefore, the frequency response from load should be removed in order to evaluate the load corresponding to the nominal frequency:

$$P_{load} = \frac{P_{measured\ load}}{1 + D\Delta f_{historic}} \tag{4.2}$$

Reliability unit commitment (RUC) is a process to ensure that there is adequate resource capacity and Ancillary Service capacity committed in the proper locations to serve ERCOT forecasted load. As the load, DC ties' flow, wind and PV production, and Ancillary Service requirements are the same as in historic day, there is no need to change the unit commitment from the historic one. It should be mentioned that slight changes in load and wind production due to frequency, as discussed above, will not affect unit commitment. Hence, in simulations the same units as in the historic day are committed at the same time of the day, and as a result, system inertia ($H.MVA$) will be equal to historic system inertia.

Another term in (4.1) is mechanical power (P_{mech}) produced by thermal generators which is affected by frequency variations due to units' governor responses and also provided regulation service. Hence, this term has to be calculated during simulation. Mechanical production of a thermal unit is in response to signals from ERCOT and also from its governor system. In order to calculate total mechanical power, the Simulink model computes these signals and the variations they make in units' outputs.

All other system settings will also be kept unchanged from historic values unless otherwise stated.

Figure 4.1 shows the Simulink model schematic. During model simulation, frequency will be determined continuously by solving the swing equation (4.1), which is represented by "Swing Equation" block in Figure 4.1. Details of all other required calculations will be discussed in Section 4.3.1 to Section 4.3.6. Finally, an overview of the model will be summarized in Section 4.3.7.

4.3.1 Security Constrained Economic Dispatch

In ERCOT, Security constrained economic dispatch (SCED) usually runs every 5 minutes and each run takes about 10-20 seconds. SCED calculates the total generation needed for the end of the upcoming 5 minutes [called generation to be dispatched (GTBD)], and distributes it among generation resources based on units' Real-Time market offers and system constraints. GTBD is a function of predicted load ramp rate [PLDRR (MW/min)] for the next 5 minutes and filtered average of total requested regulation (FAR) at

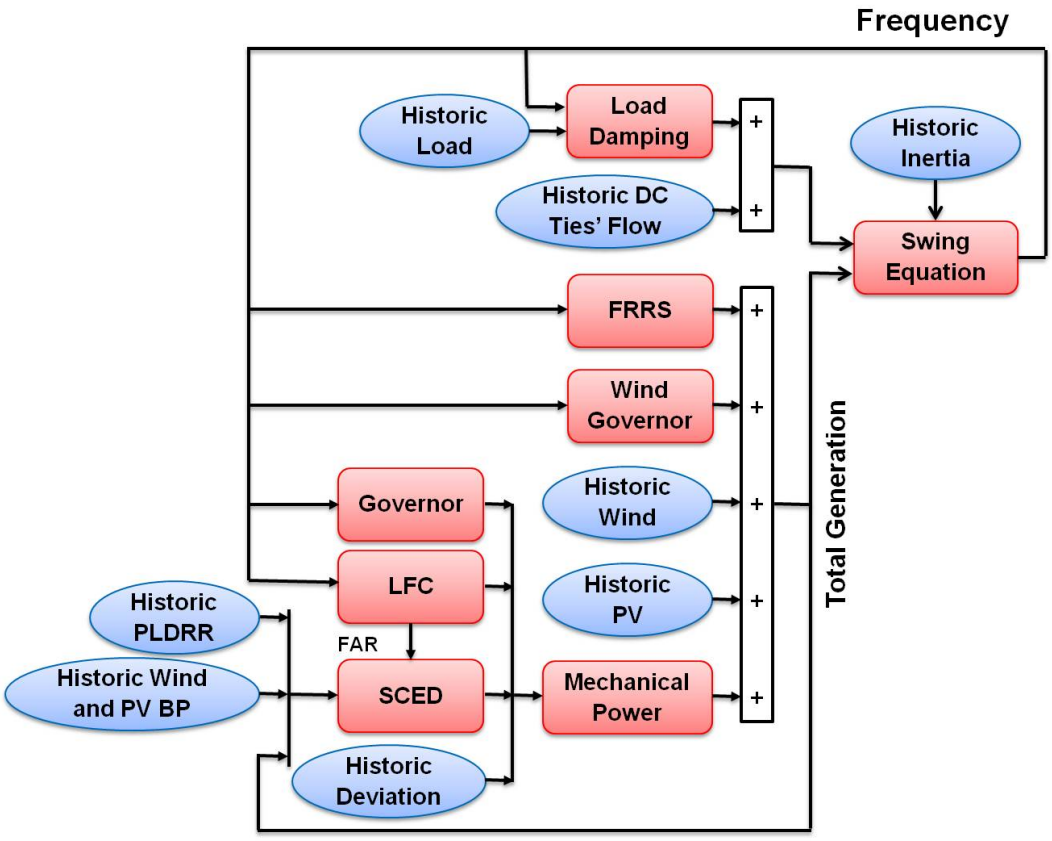

Figure 4.1: EFMAT model schematic

the time of SCED run added to total generation in the system at the time of SCED run:

$$\text{GTBD} = \text{Total Generation} + \alpha * 5 * \text{PLDRR} + \beta * \text{FAR} \tag{4.3}$$

where α and β are constants set by system operators.

As load is assumed unchanged from historic data, PLDRR will also be kept the same as historic one. However, because simulated frequency will not be the same as historic frequency, requested regulation will be different from historic one and as a result, historic SCED can not be used and GTBD has to be recalculated by the model during the simulation. Even though the model calculates requested regulation based on simulated frequency, there will not be major changes in GTBD from historic. Therefore, total calculated GTBD should still be attainable over 5 minutes by committed generation fleet. Hence, there is no need to change unit commitment from the historic one.

GTBD is shared among all units and is equal to sum of all units' base points. In SCED, wind and PV units' next interval base points are equal to their current production unless there is a need to curtail them due to transmission constraints or power balance constraint. Since load, wind and PV production are similar to historic ones and GTBD variations from historic values are minor, it is valid to assume that wind and PV curtailments will be the same as historic curtailments. Therefore, wind and PV base points are assumed unchanged from historic values, and the sum of all thermal units' base points is determined by the difference between calculated GTBD in the

Simulink model and sum of all wind and PV units' historic base points.

Calculation of thermal units' base points is represented by "SCED" block in Figure 4.1.

4.3.2 LFC System

ERCOT LFC system calculates regulation every 4 seconds. First, Area Control Error (ACE) is calculated and processed by a proportional controller with varying gain and also some other low-pass filters. Total regulation to be deployed will be equal to the filtered ACE plus total deployed regulation in previous LFC cycle. This incremental calculation is in fact similar to integral controller which is common to use in LFC calculations of other power systems. Regulation will be shared among all regulation suppliers proportionally to their responsibilities.

Also, calculated regulation will be limited to total procured capacity for the regulation service. The procured capacity for each hour of a day is equal to the regulation requirement calculated by ERCOT for that hour.

Total regulation calculation is represented by "LFC" block in Figure 4.1.

4.3.3 Governor Systems

Each generating unit has a governor, which senses frequency and controls unit's production to slow down frequency changes. In ERCOT, governor request is determined by governor droop and deadband as described in Sec-

tion 3.3 based on (3.3).

Unlike total base point that is calculated for the entire thermal generation fleet and total regulation calculation in the EFMAT model, governor request will be calculated for each unit based on its own governor deadband and droop.

Requests from thermal units' governors are represented by "Governor" block in Figure 4.1.

4.3.4 Mechanical Power

Expected mechanical power is the sum of expected responses to SCED base points, LFC signal, and governors' requests. However, there are deviations from expected mechanical power in the reality.

The rest of this section will discussed expected responses and possible deviations.

4.3.4.1 Expected Response to SCED Base Points

ERCOT expects units to ramp to their next base points, calculated by SCED, over 5 minutes[1]. Even if some units ramp faster or slower, the whole system is able to ramp to GTBD during next 5 minutes. Therefore, it is assumed that the entire committed thermal generation fleet is linearly ramping from its current output to the next total thermal generation base point over

[1]However, there are some discrepancies and lack of clarity about ERCOT expectations and what is best for measuring and modeling. Reference [54] discussed this issue.

the next 5 minutes.

SCED calculation usually starts at the beginning of each 5 minutes and 10-20 seconds later calculated base points are ready to be sent out. However, there are communication delays before units receive their base points. Thus, to calculate the expected response to SCED base points, time required to run SCED and also communication delays between ERCOT and generating units have to be considered.

4.3.4.2 Expected Response to LFC

Units offering regulation service are required to be capable of providing their offered capacity over 5 minutes if requested. As total requested regulation is shared among all regulation suppliers proportionally to their responsibilities, the model presumes that the total requested regulation will be provided with a ramp rate equal to total regulation responsibility divided by 5 minutes. This expected response to LFC signal must also consider communication delay between ERCOT and generating units.

4.3.4.3 Expected Responses to Governors

As explained before, when frequency is below nominal frequency, a unit's response to its governor request is limited to its headroom, i.e. the difference between unit's high sustainable limit (HSL) and its current output. When frequency is above nominal frequency, unit's response is limited to its legroom, i.e. the difference between a unit current output and its low

sustainable limit (LSL).

HSL and LSL of each unit are also preserved as historic data. Based on the discussions in previous parts, units' outputs during the simulation will have minor changes from the historic outputs. Hence, historic units' headroom and legroom can still be used in the model.

Governor response of each turbine is determined by the turbine's dynamic behavior. In EFMAT, each turbine is represented individually using simplified models for steam and gas turbines described in Section 3.4. Typical time constants of 0.4 second and 0.2 second are assumed for each of steam turbines and gas turbines respectively. This assumption is not in contradiction with results presented in Section 3.6 which question the validity of using typical parameter values for equivalent turbine models because EFMAT represents each turbine separately instead of replacing all turbines of a similar type with an equivalent turbine.

As discussed in Section 3.4.2, the steam turbine component of a CCGT unit usually operates in sliding pressure mode and so does not provide governor response. As a result, in order to calculate the governor request of a CCGT unit, only the capacity of its gas turbine component has to be used. In Section 3.4.2, typical ratio of gas turbine capacity to total CCGT capacity, which is two third, was assumed. However, in EFMAT model the exact ratio of gas turbine capacity to total capacity of each combined cycle unit is used.

4.3.4.4 Deviation

Historic mechanical power produced during a selected day can be computed based on:

$$P_{mech} = 2\,H.MVA\,\frac{d\Delta f}{dt} - (P_{wind} + P_{PV} + P_{FRR} - P_{ties} - P_{measured\ load}) \quad (4.4)$$

where all data are historic ones. As measured load already includes load damping effect, there is no need to add load frequency response.

For the selected day, expected mechanical power is calculated as the sum of expected responses to historic SCED base points, historic LFC signal, and historic governors' requests as defined in previous sections.

Calculation shows that there is major deviation between historic and expected mechanical power during any historic day. This deviation varies between -2% and +2% of expected mechanical power throughout the day mostly due to a few units not behaving as expected, especially by not following their base points[2].

The proposed solution is to treat power deviation as a special feature of the system at each particular time of a day. In the model, unit commitments are the same as historic day and calculated GTBD and units' base points during simulations will not have major differences with historic ones. As mentioned before, deviations are mostly due to a few units not following their base points. It is assumed that those few units will behave the same as they did historically in the simulations. Hence, deviations from the expected response of

[2]Confirmed by ERCOT system operators.

the thermal generation fleet can be assumed equal to the calculated deviations based on historic data. Therefore, in the Simulink model, mechanical power is calculated as the sum of expected responses and historic power deviation, represented in "Mechanical Power" block in Figure 4.1.

4.3.5 Wind Governor Response

The majority of wind units in ERCOT are required to have governors in service. In this model, wind governor request is calculated based on wind unit's governor characteristics using (3.3). A wind unit's output is usually equal to its HSL unless it was curtailed by SCED. Therefore, for each wind unit, headroom is assumed zero except for SCED cycles when unit's output is below its HSL which means the unit was curtailed. Wind governor response calculation is represented by "Wind Governor" block in Figure 4.1.

4.3.6 Communication Delay

All generation units have to telemeter their output to ERCOT every 4 seconds. ERCOT also sends signals including units Updated Desired Base Point and regulation request to each unit every 4 seconds. All of these communications are subject to delays which have to be considered in the model. One-way communication delay between ERCOT and units is typically 6 to 8 seconds. EFMAT assumes 7 seconds for all units. However, for the resource providing FRRS during 2013-2016, one-way communication delay has been about 15 seconds which is considered in EFMAT validation phase. For the

rest of the study, delay for fast-responding resources is assumed similar to other units.

4.3.7 EFMAT Simulink Model Overview

As mentioned previously, EFMAT model with schematic shown in Figure 4.1 is built in Simulink. Considering the objectives of this study, historic values of some system aspects are used in simulations. The other aspects are calculated during simulations.

Table 4.1 provides a list of items which are calculated during each simulation, and those which are kept the same as their historic values.

Table 4.1: List of items which are kept as historic or calculated

To be kept as historic	To be calculated
System inertia	Frequency
Load and PLDRR	Deployed regulation and FAR
DC ties' flow	Deployed FRRS
Wind and PV productions	Wind governor response
Wind and PV base points	GTBD
Deviation	Thermal mechanical power

In each simulation step[3], governor requests of all thermal units are calculated. Every 4 seconds, LFC system determines required conventional regulation service and filtered average regulation (FAR). Every 5 minutes, SCED calculates total base points of thermal units based on total generation

[3]For each model simulation, the solver maximum step time is set to 0.5 second.

in the system, FAR calculated by LFC, historic PLDRR, and historic wind and PV units' base points. Sum of expected response of thermal units to governor requests, requested regulation, and SCED base points will be added to historic deviation in order to calculate total thermal mechanical power in each simulation step.

Total produced mechanical power added to historic production of wind and PV units plus total wind units' governor response is equal to total generation in the system.

Special design of FRRS will determine the output of fast-responding resources every 4 seconds. Finally, frequency will be calculated in every simulation step by solving the swing equation using total generation, provided FRRS, historic load, historic DC ties' flow, and historic system inertia.

4.4 EFMAT Post-Processing

Finally, simulation results will be analyzed in the post-processing part. One of the tasks of this part is to calculate Control Performance Standard 1 (CPS1) which is an index defined by NERC to assess an interconnection performance in controlling frequency [19]. CPS1 is calculated based on one-minute average of ACE. To meet the compliance requirement of NERC, CPS1 score over a rolling 12 months should be at least 100% [35]. It should be mentioned that ERCOT has been granted waiver by NERC for CPS2 (another NERC-defined index) [18].

As ERCOT is a single balancing authority, CPS1 is calculated as:

$$\Delta f_{\text{ clock-minute}} = \frac{\Sigma\, \Delta f_{\text{ sampling cycles in clock-minute}}}{n_{\text{ sampling cycles in clock-minute}}} \tag{4.5}$$

$$\text{CF}_{\text{ clock-minute}} = \frac{(\Delta f_{\text{ clock-minute}})^2}{(\epsilon_1)^2} \tag{4.6}$$

$$\text{CF}_{\text{ 24-hours}} = \frac{\Sigma\, \text{CF}_{\text{ clock-minute}}}{n_{\text{ clock-minute in 24-hours}}} \tag{4.7}$$

$$\text{CPS1} = 100\ (2 - \text{CF}_{\text{ 24-hours}})\ \% \tag{4.8}$$

In the above equations, Δf is frequency deviation from nominal frequency in Hz, "CF" stands for Compliance Factor, and ϵ_1, a constant derived from a targeted frequency bound, is 30 mHz for ERCOT [19].

4.5 EFMAT Verification and Validation

By conducting several tests, GTBD calculation, LFC logic, and FRRS logic implemented in the EFMAT model are verified using historic operational data. All these features of the system are well represented in the model.

The whole model is also validated for four weekdays from different seasons of 2014 which did not have any contingency events. Required historic data are gathered for these days, reformatted by EFMAT pre-processing part, and used by EFMAT model to simulate frequency over each 24-hours.

As discussed in Section 4.3.4.4, there is deviation between total expected mechanical power, as defined in EFMAT, and total historic mechanical power at any time in the system. This power deviation is treated as special

feature of the day. For validation, the model is run two times for each day, one time assuming zero deviation and one time with the assumption that deviation is the same as historic power deviation. The resulting frequency of each scenario is sampled every 4 seconds and compared to the historic frequency with respect to frequency profile, 5th and 95th percentile, and CPS1 for the whole day.

In order to compare frequency profiles, frequency histograms are plotted in 1 mHz bins. For each day, histograms of simulated frequencies (green and blue plots) are transparently plotted over the histogram of historic frequency (black plot). Darker green or darker blue areas show the overlap of simulated and historic frequencies histograms.

In the rest of this section, the results of validation process for the four selected days will be presented and discussed.

4.5.1 Model Validation Results for January 17, 2014

Results of model validation for January 17, 2014 is presented in Figure 4.2 and Table 4.2.

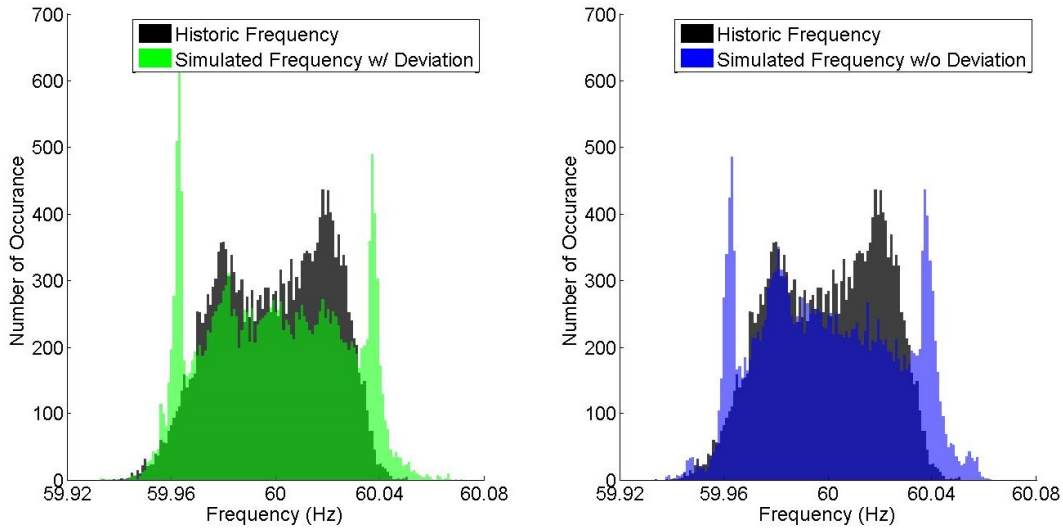

Figure 4.2: Histograms of historic frequency and simulated frequencies with/without deviation for January 17, 2014

Table 4.2: Results of model validation for January 17, 2014

	5^{th} Percentile (Hz)	95^{th} Percentile (Hz)	CPS1
Historic Frequency	59.9650	60.0310	157%
Simulated Frequency w/ Deviation	59.9612	60.0388	140%
Simulated Frequency w/o Deviation	59.9610	60.0408	142%

4.5.2 Model Validation Results for April 23, 2014

Results of model validation for April 23, 2014 is presented in Figure 4.3 and Table 4.3.

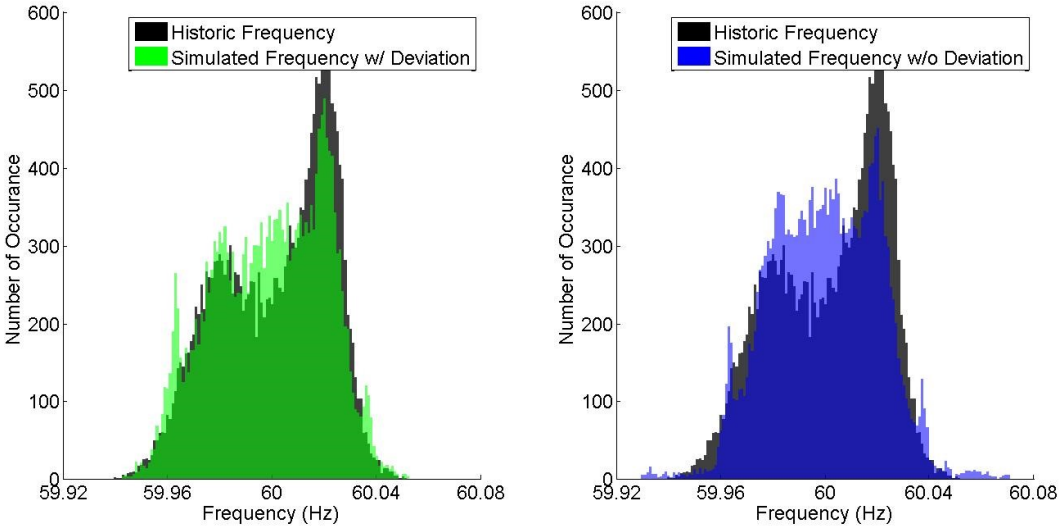

Figure 4.3: Histograms of historic frequency and simulated frequencies with/without deviation for April 23, 2014

Table 4.3: Results of model validation for April 23, 2014

	5^{th} Percentile (Hz)	95^{th} Percentile (Hz)	CPS1
Historic Frequency	59.9650	60.0290	156%
Simulated Frequency w/ Deviation	59.9629	60.0298	158%
Simulated Frequency w/o Deviation	59.9659	60.0306	164%

4.5.3 Model Validation Results for July 15, 2014

Results of model validation for July 15, 2014 is presented in Figure 4.4 and Table 4.4.

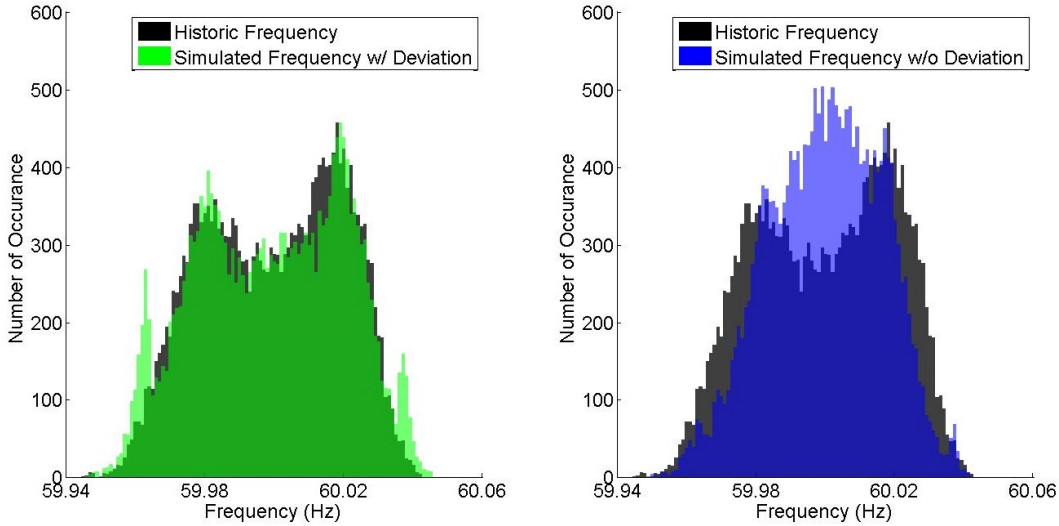

Figure 4.4: Histograms of historic frequency and simulated frequencies with/without deviation for July 15, 2014

Table 4.4: Results of model validation for July 15, 2014

	5^{th} Percentile (Hz)	95^{th} Percentile (Hz)	CPS1
Historic Frequency	59.9676	60.0290	162%
Simulated Frequency w/ Deviation	59.9634	60.0310	156%
Simulated Frequency w/o Deviation	59.9726	60.0248	176%

4.5.4 Model Validation Results for October 23, 2014

Results of model validation for October 23, 2014 is presented in Figure 4.5 and Table 4.5.

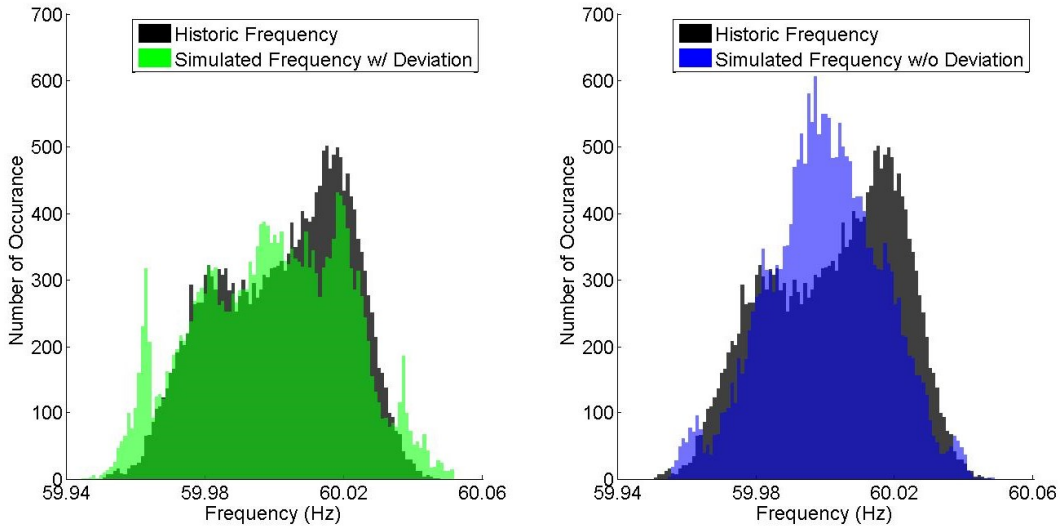

Figure 4.5: Histograms of historic frequency and simulated frequencies with/without deviation for October 23, 2014

Table 4.5: Results of model validation for October 23, 2014

	5^{th} Percentile (Hz)	95^{th} Percentile (Hz)	CPS1
Historic Frequency	59.9710	60.0290	166%
Simulated Frequency w/ Deviation	59.9627	60.0334	155%
Simulated Frequency w/o Deviation	59.9720	60.0261	176%

4.5.5 Discussion of Model Validation Results

The results of model validation tests show that the model with considering deviation well represents the reality with one particular exception relating to the occurrence numbers of frequency values near the governor deadband boundaries.

To explain the discrepancy, note that in all validation tests, the data is taken from 2014 when most of the governor deadbands were set at 36 mHz. In the histograms of simulated frequencies, there are spikes near the governor deadbands. In the real world, at any time, frequencies in different physical locations of the system are not exactly the same, and each governor may see different frequency and also, may have measurement errors. As a result, even governors with the same deadbands may not be activated at the same time. However, EFMAT model assumes uniform frequency in the system and it does not contain any physical location information. So, a hypothesis is that assuming identical frequency in all locations causes governors to be activated at the same time and produces spikes around governors' deadbands.

Experiments were done in order to remove those spikes, such as adding random variables to governor deadbands, changing governor dynamic model parameters, or modifying other model assumptions. However, none of them were able to remove spikes without deteriorating other characteristics. Also, none of those modifications resulted in CPS1 significantly closer to historic CPS1. So, a firm conclusion was not reached in this study regarding the spikes in the histograms of simulated frequencies.

Chapter 5

Study ERCOT Fast-Responding Regulation Service (FRRS)

5.1 Introduction

In ERCOT, fast-responding regulation service (FRRS) is a subset of regulation service from resources capable of ramping to their full outputs within 60 cycles of either receipt of ERCOT signal or detection of a trigger frequency autonomously.

FRRS is designed to respond first, ahead of conventional regulation, and help slow down the frequency decay while other resources start to provide conventional regulation. However, the duration of FRRS response is limited. Resources providing FRRS (Up and Down) must be able to continuously remain deployed for up to 8 minutes with 95% or more of their responsibility for successful qualification [59].

The objective of this chapter is to evaluate the effectiveness of ERCOT FRRS. In the rest of this chapter, logic designed by ERCOT to deploy FRRS will be introduced in Section 5.2. Then, the study method and the results of two different scenarios will be presented in Section 5.3.

5.2 ERCOT Logic for FRRS Deployment

ERCOT FRRS was first introduced in a pilot project [55] which was conducted from January 2013 to February 2014. Since March 2014, FRRS was implemented as an official subset of regulation service.

ERCOT designed a logic for FRRS deployment during the pilot project based on participating resources and their capabilities [59]. In this logic, different bands are determined for frequency (shown in Figure 5.1) and two events are defined.

- High frequency event: when frequency enters a High Trigger Band, a high frequency event starts. During a high frequency event, if frequency decreases to and stays in a Reset Band for 12 seconds consecutively, or goes beyond Low Reset Level, the high frequency event ends.
- Low frequency event: when frequency enters a Low Trigger Band, a low frequency event starts. During a low frequency event, if frequency increases to and stays in a Reset Band for 12 seconds consecutively, or goes above High Reset Level, the low frequency event ends.

During an event, any time frequency entered a trigger band which was worse than any other band entered previously during the current event, a deployment will start and continue for at most 1 minute even if frequency improves to a better band. For any high-frequency event, FRRS-DN will be deployed which means a resource providing FRRS will consume electricity as a

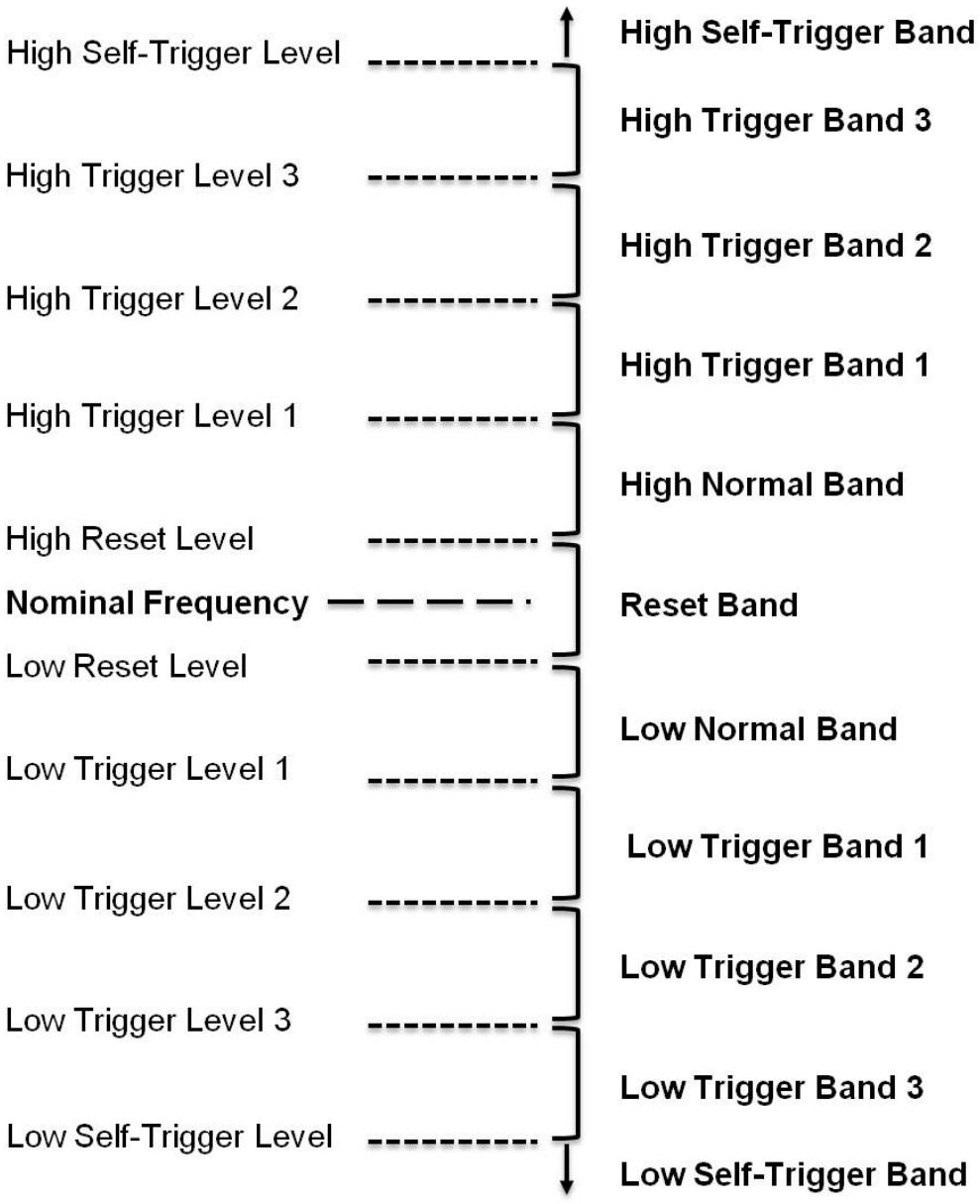

Figure 5.1: Frequency Trigger Levels and Bands defined by ERCOT FRRS deployment logic

Table 5.1: ERCOT FRRS deployment logic settings

	ERCOT Settings (Hz)	Proposed Settings (Hz)
Reset Level	60 ± 0.01	
Trigger Level 1	60 ± 0.03	60 ± 0.014
Trigger Level 2	60 ± 0.04	60 ± 0.024
Trigger Level 3	60 ± 0.05	60 ± 0.034
Self Trigger Level	60 ± 0.09	

load resource. For any low-frequency event, FRRS-UP will be deployed which means a resource providing FRRS will generate electricity as a generation resource. After one minute, deployment will be recalled in 3 equal steps. Each step lasts 12 seconds. Also, when an event ends, any deployment is recalled in 3 steps. However, if a high event starts in the middle of a low event or vice versa, any required recall will be done in one step. If frequency enters a self-trigger band, FRRS has to be deployed autonomously without waiting for the ERCOT signal.

Table 5.1 shows ERCOT settings for different frequency levels during 2014 which are still in-use. Also, this table contains the proposed settings in this paper which will be discussed in Section 5.3.1. As defined in 2014, FRRS deployment in trigger bands 1, 2, and 3 will respectively be 40%, 70%, and 100% of total FRRS responsibility. For self-trigger band, deployment is also 100%.

5.3 ERCOT FRRS Study

The main purpose of this chapter is to study the effectiveness of using fast-responding resources to control frequency in ERCOT. For this purpose, EFMAT is used to study historic days selected from 2014 weekdays that did not have any contingency events. All system settings are kept the same as historic days except:

- Fast-responding resource participation: in the study, the capacity of fast-responding resources procured for FRRS is varied from historic because the purpose of the study is to investigate the effects of different procured capacity for FRRS on system frequency control performance. It's assumed that procured capacity for FRRS UP is fixed all through the day and equal to procured capacity for FRRS DN .

- Governor setting: by the beginning of year 2016, all generation units had to be compliant with a NERC approved standard from Texas Reliability Entity, BAL-001-TRE-1 [24]. One of the requirements of this standard is to narrow governor deadband to 17 mHz for most units. In this study, 2016 governor settings are used.

- Regulation requirements: from 2016, as a result of changes in governors' settings, the calculation method of total regulation requirements has also changed. Thus, regulation requirements for the test days in 2014 are recalculated based on 2016 method and used in the study. Details of both 2014 and 2016 methods are included in Appendix B.

As FRRS is a subset of regulation service, FRRS responsibility plus total regulation responsibilities from conventional generators has to be kept equal to total regulation responsibility. For each day, a case with zero FFRS responsibility is considered as a base case. For all other cases, FRRS procured capacity is gradually increased and total conventional regulation responsibility is adjusted accordingly.

In order to evaluate the effects of increased FRRS responsibility, CPS1 is calculated for each 24-hours simulation. Increasing CPS1 compared to base case shows that replacing conventional regulation by FRRS improves system frequency control performance. Decreasing CPS1 compared to base case shows poor performance of FRRS compared to conventional regulation.

The study is done for two different scenarios which will be discussed in the following sections.

5.3.1 Scenario I: Current ERCOT logic for FRRS deployment

In this scenario, ERCOT defined logic described in Section 5.2 is used to deploy FRRS. One day from each season of 2014, a total of 4 days, was selected for this study. For each day, frequency was simulated using EFMAT for different FRRS procured capacities and CPS1 is calculated over 24 hours. Figure 5.2 to Figure 5.5 show calculated CPS1 versus FRRS capacity in solid line for each day. As the plots depict, using ERCOT FRRS deployment logic with ERCOT designed trigger levels results in a lower CPS1 score than base case CPS1 (dotted horizontal lines in Figure 5.2 to Figure 5.5) for all days.

When ERCOT was designing FRRS trigger levels, most generating units had 36 mHz governor deadbands. However, in this study, governor deadbands are based on 2016 requirements which are 17 mHz for most of units. With these narrower deadbands, frequency is in a narrower range, and ERCOT FRRS trigger levels do not provide sufficient opportunity for FRRS to be deployed, which may result in FRRS not being as effective as conventional regulation. To test this hypothesis, narrower trigger levels, shown in Table 5.1, are proposed and tested by repeating all simulations using these levels. Based on the results, shown by dashed lines in Figure 5.2 to Figure 5.5, CPS1 is improved compared to ERCOT designed trigger levels, but still no improvement compared to base case CPS1 except in October 23 for FRRS capacity less than 20 MW. However, even in October 23 the maximum improvement in CPS1 is only about 1 percentage point.

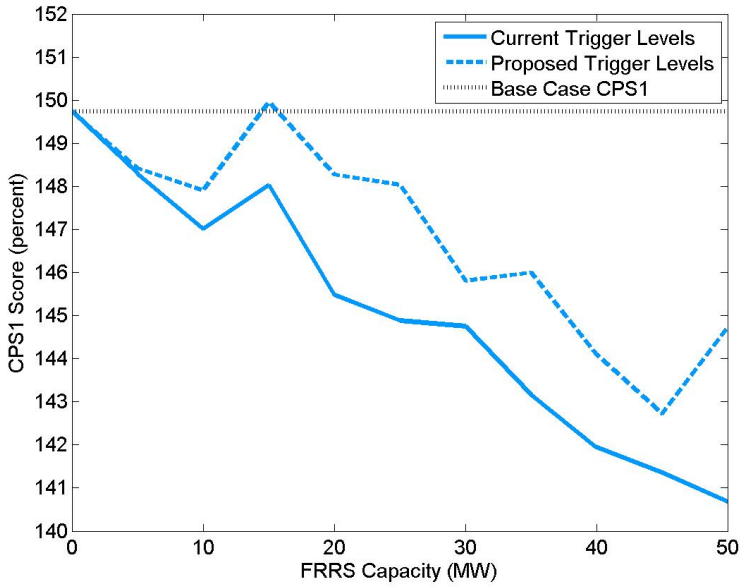

Figure 5.2: Results of scenario I for January 17

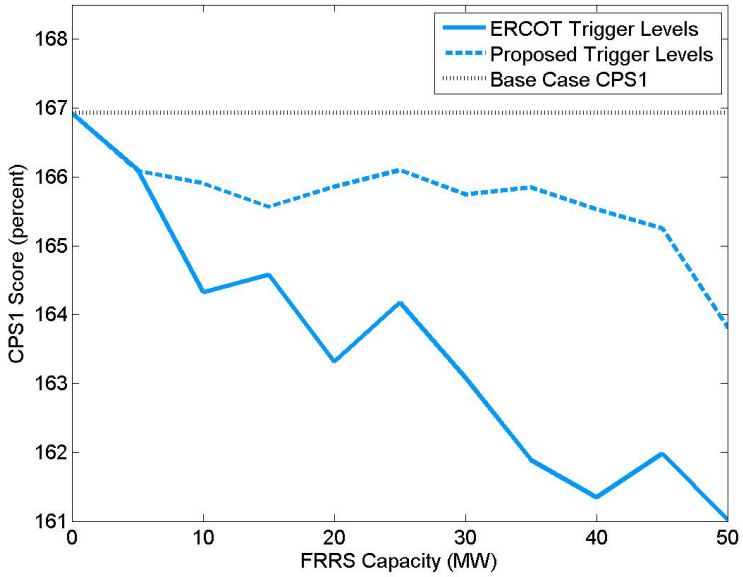

Figure 5.3: Results of scenario I for April 23

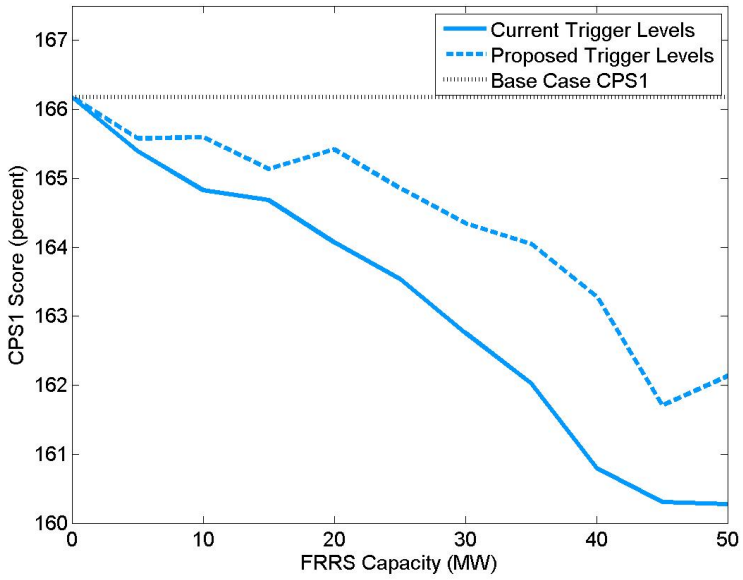

Figure 5.4: Results of scenario I for July 15

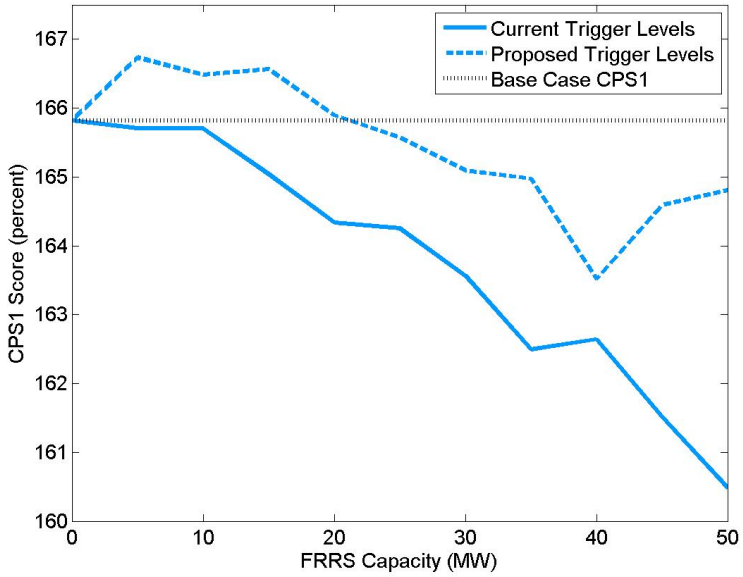

Figure 5.5: Results of scenario I for October 23

5.3.2 Scenario II: Energy Limited Logic

Based on results presented in previous section, replacing conventional regulation by FRRS and deploying FRRS based on ERCOT designed logic deteriorates CPS1. Even modifying FRRS trigger levels to the proposed narrower bands did not result in improved CPS1 scores compared to the base case.

Another issue with ERCOT logic may be the limited deployment time which is up to 1 minute at each trigger band. In this scenario, a new "energy limited" deployment logic is proposed and tested. This logic is the same as ERCOT logic except the deployment is not limited by time. Instead, FRRS will be kept deployed as long as it is needed and it will be recalled whenever the frequency event ends as defined in Section 5.2. The logic also keeps track of total energy produced (as FRRS UP) or consumed (as FRRS DN) by the storage system. Whenever the stored energy reaches the minimum level, the logic will recall FRRS completely and wait till the next chance to deploy FRRS DN and thus, charge the storage. Also, whenever the stored energy reaches the maximum level, the logic will recall FRRS completely and wait till the next chance to deploy FRRS UP and thus, discharge the storage.

As described in Section 5.1, a FRRS provider is required to be able to store energy almost up to its MW responsibility times 8 minutes. Consistent with this requirement, in the proposed energy limited logic, the maximum level of stored energy is assumed equal to FRRS responsibility times 7 minutes and the minimum energy level is assumed equal to FRRS responsibility times one

minute. These assumptions prevent full charging or deep discharging of storage system.

Results of this scenario for four selected days are represented in Figure 5.6 to Figure 5.9. As the results show, deploying FRRS with energy limited logic using ERCOT trigger levels still deteriorates CPS1. However, modifying trigger levels to the proposed ones results in CPS1 improvements compared to the base case with no FRRS.

Although proposed logic resulted in CPS1 improvements, this logic also has drawbacks. One of the issues is that with the proposed narrower trigger bands, frequency rapidly goes from a high frequency event to a low frequency event (or vice versa). This rapid changes will result in frequent alteration between deploying FRRS UP and FRRS DN that may adversely affect the storage lifetime.

In the LFC system, calculated ACE shows the required MW to perfectly control frequency. That is why deployed regulation is determined based on ACE. Different from the LFC logic, the proposed FRRS logic determines the amount of FRRS deployment as a percentage of FRRS procured capacity regardless of required MW to control frequency. This will result in deploying different MW of FRRS for the same frequency value when different FRRS capacity is procured. In the next chapters, we will propose and test several FRRS deployment logics which are based on ACE calculation.

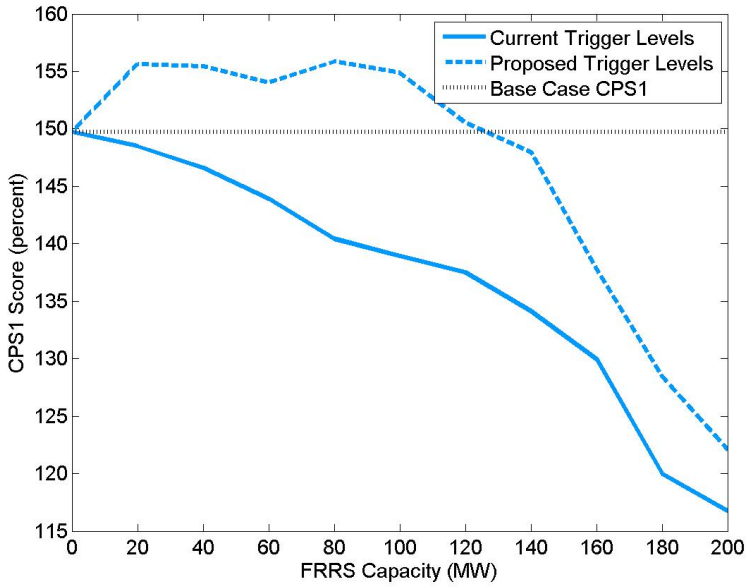

Figure 5.6: Results of scenario II for January 17

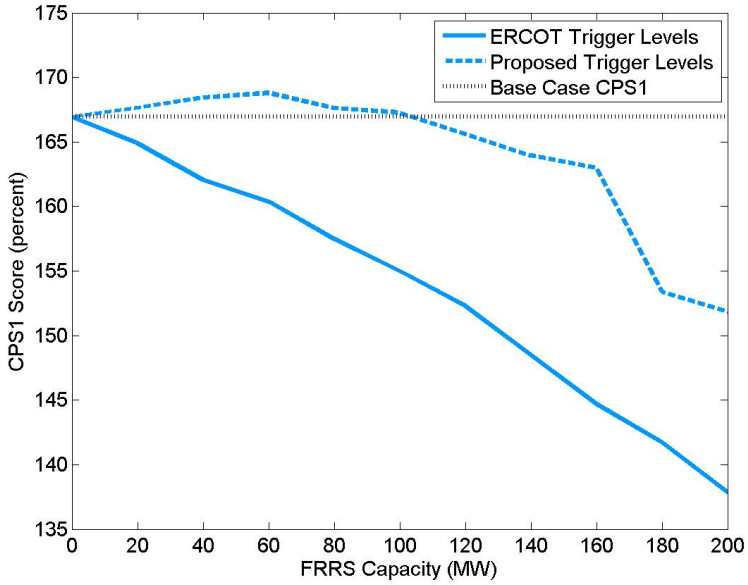

Figure 5.7: Results of scenario II for April 23

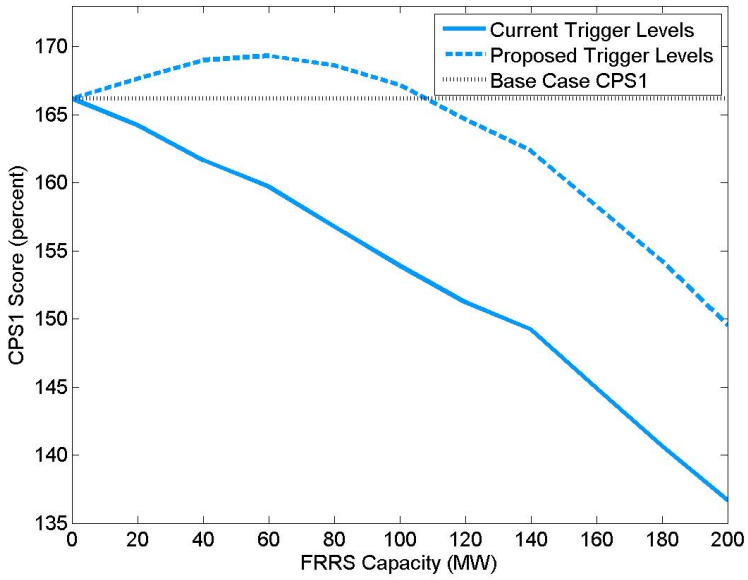

Figure 5.8: Results of scenario II for July 15

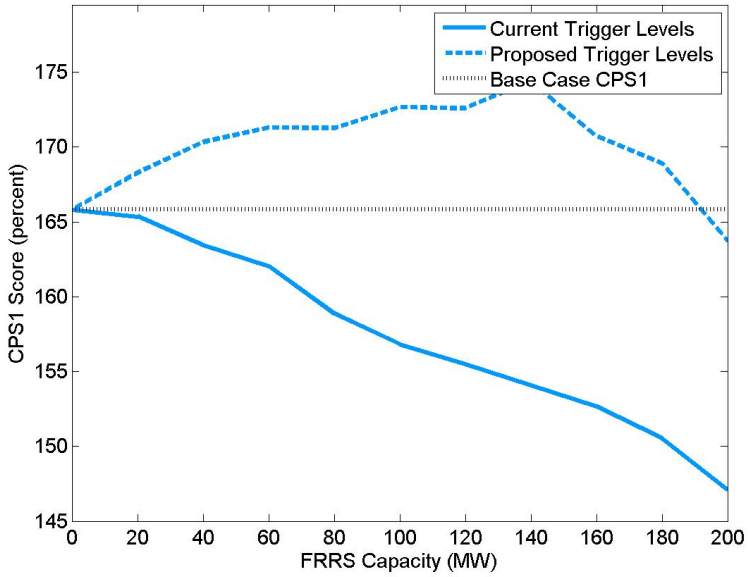

Figure 5.9: Results of scenario II for October 23

Chapter 6

Deploying FRRS Using ACE-Derived Signals

6.1 Introduction

The results of ERCOT FRRS study presented in Section 5.3 showed that fast regulation service can be helpful or harmful in controlling frequency. In fact, the results revealed the effects of deployment logic on the level of FRRS effectiveness. Thus, successful integration of fast regulation service requires a well-designed logic, which provides enough opportunity for fast resources to improve system frequency control performance.

The common approach to design such a logic is to create a signal derived from the area control error (ACE), similar to conventional LFC signal. This approach has been employed in several power systems across North America. The objective of this chapter is to test this approach for FRRS deployment in the ERCOT system using EFMAT developed in Chapter 4.

In the rest of this chapter, a summary of fast regulation service and its deployment signal in several power markets will be presented in Section 6.2. Then, Section 6.3 will explain the methodology of studying the effectiveness of ERCOT FRRS deployed based on ACE-derived signals and also clarify the assumptions. Section 6.4 is dedicated to several study scenarios using LFC

conventional signal to deploy FRRS and Section 6.5 is dedicated to several study scenarios using a fast-dynamic signal to deploy FRRS.

6.2 Fast-Responding Regulation Service in North America Power Markets

In 2007, FERC directed all RTOs and ISOs in its jurisdiction through its Order Number 890 [16] to reduce entry barriers of non-generation technologies to power markets and specifically, allow them to provide ancillary services [15, 53].

Consequently, the New York ISO (NYISO) introduced a class of resources known as Limited Energy Storage Resources (LESRs) and supported their integration by developing new market rules and market software in 2009 [53]. Similarly, during 2009, the Midcontinent ISO (MISO) worked on the design of its market to incorporate Stored Energy Resources (SERs) into the regulation market [14, 45]. Also, California ISO (CAISO) has developed pilot projects to study participation of these new technologies in its regulation market [14]. Finally, in CAISO, LESRs are categorized as Non-Generating Resources (NGR) and the market design is modified accordingly to enable participation of this type of resources in the regulation market [8].

NYISO, MISO, and CAISO use the conventional LFC signal, derived from ACE, to deploy regulation service provided by storage resources. As the conventional LFC signal has slow dynamics, storage resources may become fully charged or fully discharged by providing regulation service for even a rela-

tively short period of time. Therefore, NYISO, MISO, and CAISO incorporate State of Charge (SoC) of storage resources to determine regulation base point (or energy dispatch) and regulation capacity of a storage resource [15, 44, 74]. MISO has also proposed a new regulation deployment scheme called "AGC Enhancement" in order to take more advantage of fast-responding resources [45].

Conventional LFC signal is designed based on slow ramping capabilities of thermal generators. Thus, using this signal to deploy fast-responding regulation service has been challenged in some electricity markets. Instead, a new signal has been designed considering capabilities and limitations of energy storage systems. Such signals are developed and utilized by the RTO of the Pennsylvania-New Jersey-Maryland Interconnection (PJM) and also, the ISO New England (ISO-NE).

Since 2009, energy storage systems have participated in the PJM regulation market [5]. PJM LFC system develops two regulation deployment signals, which can be chosen to be followed by each regulation provider. RegA signal is the traditional PJM regulation signal that has a slow dynamic. RegD signal designed specifically for energy storage systems has a fast dynamic [5, 74].

In ISO-NE, storage systems are classified as Alternative Technology Regulation Resources (ATRRs) [74]. In addition to the conventional regulation signal, the LFC system of ISO-NE develops two other signals. The first of these signals is called Energy Neutral Continuous (ENC) and is similar to the PJM RegD signal. The second signal is called Energy Neutral Trinary

(ENT). Trinary means that the dispatch is either full power charge, full power discharge, or midpoint. Therefore, a resource following ENT will be sent to its Regulation High Limits, Regulation Low Limits, or Regulation Midpoints (i.e. (Regulation High Limit minus Regulation Low Limit)/2) [34].

In the next sections, we will test similar approaches used in the mentioned markets for the ERCOT system.

6.3 Study Methodology and Assumptions

The main purpose of this chapter is to study the effectiveness of ERCOT FRRS deployed based on ACE-derived signals. For this purpose, EFMAT is used to study historic days selected from 2014 weekdays that did not have any contingency events. Similar to the study described in Section 5.3, all system settings are kept the same as historic days except for fast-responding resource participation, governors setting, and regulation requirements. Please refer to Section 5.3 for details.

In this study, FRRS responsibility plus total regulation responsibility from conventional generators is kept equal to total regulation requirements. For each day, the base case has zero FFRS responsibility. Other cases are constructed by increasing FRRS responsibility with 20 MW increments up to 200 MW. For each case, total conventional regulation responsibility is also adjusted down accordingly.

We also assumed that there is one storage resource providing both

FRRS UP and FRRS DN. The procured capacity for both services is fixed throughout the day and equal to each other.

For the storage system, time of charge (ToC) is defined as the required time for stored energy to increase from minimum allowable level to maximum allowable level while the storage is charging at a level equal to its FRRS DN responsibility. With similar definition, time of discharge can also be determined for the storage system. In this study, time of charge and discharge are assumed equal and for each scenario, three different options for time of charge are tested:

- 6 minutes: based on ERCOT requirements as described in Section 5.3.2,
- 15 minutes: based on most other markets requirements [74], and
- unlimited: means storage has the capability to store unlimited amount of energy and thus, it never fails to provide requested regulation service.

Another term that needs to be defined is failure time. Whenever stored energy is at maximum allowable level, the storage system cannot provide FRRS DN. Thus, if LFC asks for FRRS DN in this situation, the storage will fail to respond and its output becomes zero. Similarly, whenever stored energy is at minimum allowable level, the storage system cannot provide FRRS UP. Thus, if LFC asks for FRRS UP in this situation, the storage will fail to respond and its output becomes zero. In this study, total failure time is defined as the sum of the duration of these situations when storage fails to provide the requested service.

It should also be mentioned that the storage is assumed half-charged at the beginning of the day. This means that the initial level of storage charge is assumed at the midpoint, which is equal to the sum of maximum allowable level and minimum allowable level divided by two. Therefore, at the beginning of each day, storage have the capability of providing both FRRS UP and DN.

6.4 Using Conventional Regulation Signal to Deploy FRRS

As described in Section 2.4, required regulation to be deployed is determined by LFC system based on the area control error (ACE). For interconnected systems, ACE is calculated for each balancing area based on a linear combination of frequency deviation and the deviation of total interchange with other areas from its scheduled value. A single balancing authority, such as ERCOT, does not have interchange with other balancing areas. Therefore, ACE will be simplified as $10\beta\Delta f$, where Δf is frequency deviation from its nominal value and β is frequency bias in MW/0.1Hz, which depends on the MW size of the balancing area [38].

LFC system develops a signal by processing ACE with various filters and controllers. The special design of the processing procedure considers the slow ramping capabilities of thermal generators. Some power markets use this conventional regulation signal to deploy fast-responding regulation too.

In the ERCOT LFC system described in Section 4.3.2, ACE is fed to a proportional controller with varying gain. The controller output will be

processed by low-pass filters to determine required regulation to be deployed.

In some markets, such as ERCOT, calculated regulation is shared among providers proportionally to their responsibilities. However, in some other markets, such as MISO, regulation is allocated to providers based on their ramp rate capability. One of the options MISO proposed in its AGC Enhancement scheme is to deploy and undeploy fast-responding resources ahead of other regulation providers to better utilize these resources [45].

We already tested different logics for ERCOT FRRS deployment in scenarios I and II discussed in Chapter 5. In the rest of this section, we will introduce scenarios III and IV in order to test ERCOT FRRS deployment by using conventional regulation signal along with two discussed regulation allocation methods.

6.4.1 Scenario III: Conventional Regulation Signal with Proportional Allocation Method

In scenario III, FRRS is treated the same as conventional regulation. LFC determines total required regulation and share it among all conventional and storage resources proportionally to their responsibilities.

As an example of this scenario, Figure 6.1 shows deployment signals during first three hours of April 23 simulated by EFMAT. Conventional regulation signal is the total deployment signal for thermal generators and FRRS signal is the deployment signal for a storage resource with FRRS responsibility of 40 MW. It can easily be seen that FRRS provider is treated exactly the

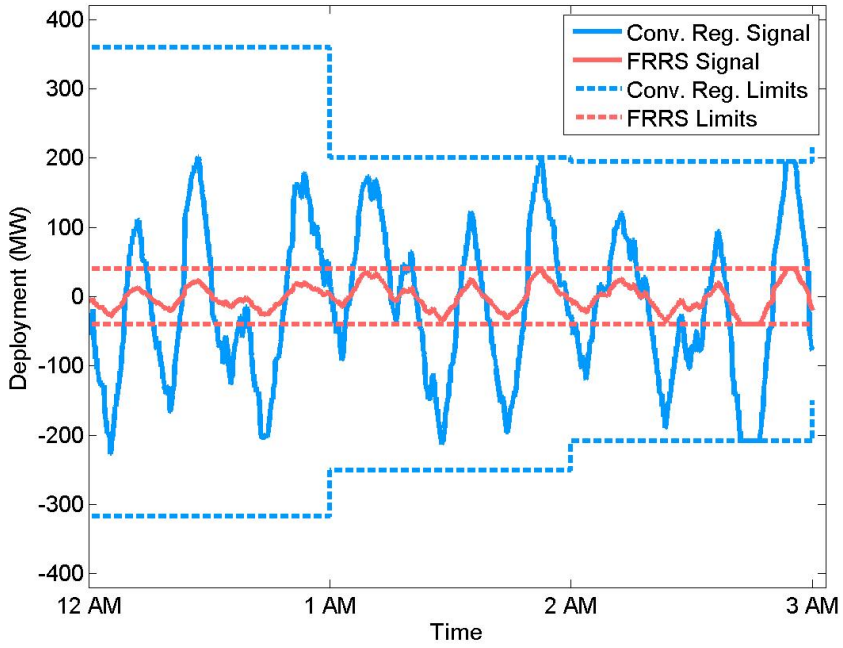

Figure 6.1: Deployment signals based on scenario III during first three hours of April 23

same as conventional regulation providers and required regulation is shared proportionally at any time.

In this scenario, whenever storage cannot respond to the signal due to being at maximum or minimum allowable level of stored energy, its output will become zero and storage will fail to provide the requested service. Traditional LFC methodology does not consider the state of charge (SoC) of storage. Thus, storage failure will not affect regulation deployments of other resources. In order to alleviate the adverse effects of storage failures, the LFC methodology can be modified to consider storage SoC and try to compensate storage

failures by adjusting regulation deployments of other resources. In the modified method, LFC first determines required FRRS service. Then, based on storage SoC, if storage is unable to provide required FRRS, LFC will send zero request to storage and share the required FRRS among thermal generators if they have enough capacity to provide it.

EFMAT is run for four selected weekdays from different seasons of 2014, using the LFC methodology of scenario III to deploy regulation and assuming a storage resource with 6 minutes, 15 minutes, and unlimited ToC. Also, modified LFC methodology of scenario III, which considers SoC, is tested for each selected day assuming a storage resource with 6 minutes and 15 minutes ToC. CPS1 score of the whole day and the storage total failure time during the day is calculated for different FRRS participation levels.

To calculate storage total failure time, we need to define storage failure. With original LFC that does not consider storage SoC, storage failures happen when the storage cannot respond to FRRS signal due to its energy limitations. However, when LFC is modified to consider storage SoC, FRRS signal will be set to zero whenever SoC is at its limits. Thus, storage will never fail to provide requested FRRS. In this case, storage failure refers to the condition when SoC is at one of its limits and LFC is forced to adjust FRRS signal to zero.

The results will be presented and discussed in the following sections.

6.4.1.1 Results of Scenario III for January 17

Figure 6.2 and Figure 6.3 show the results of scenario III for January 17.

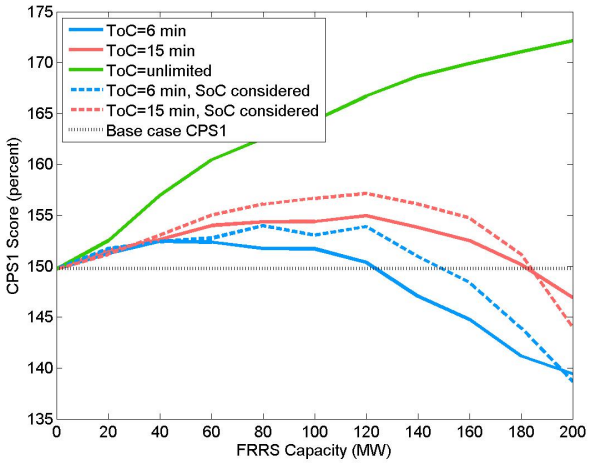

Figure 6.2: CPS1 results of scenario III for January 17

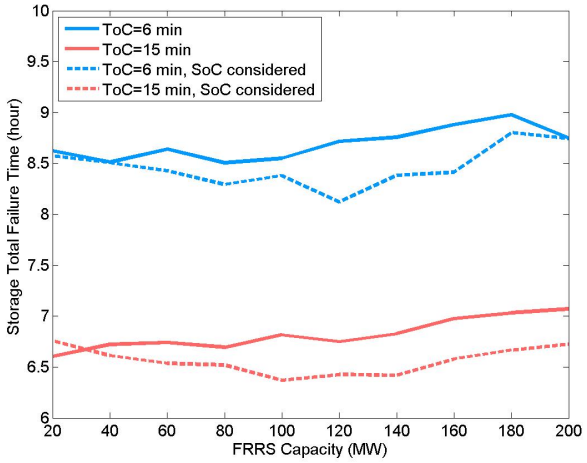

Figure 6.3: Storage failure time in scenario III for January 17

6.4.1.2 Results of Scenario III for April 23

Figure 6.4 and Figure 6.5 show the results of scenario III for April 23.

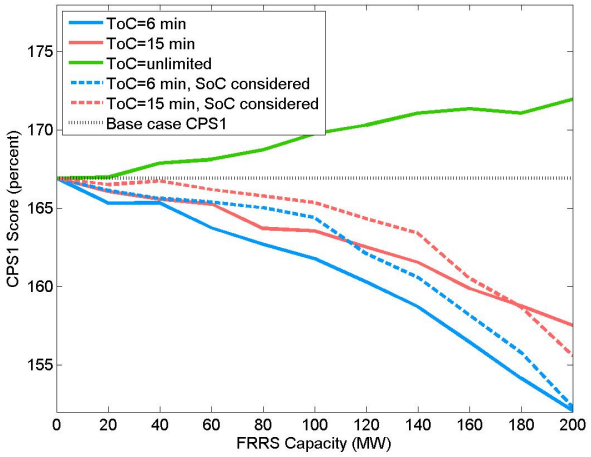

Figure 6.4: CPS1 results of scenario III for April 23

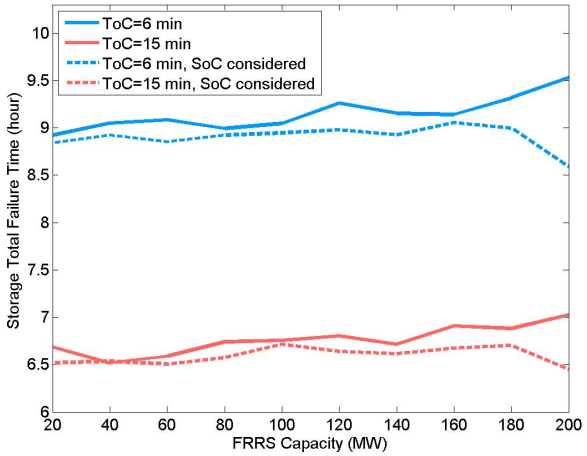

Figure 6.5: Storage failure time in scenario III for April 23

6.4.1.3 Results of Scenario III for July 15

Figure 6.6 and Figure 6.7 show the results of scenario III for July 15.

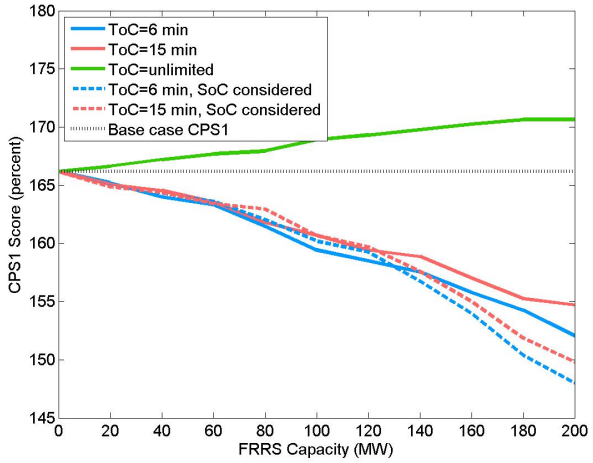

Figure 6.6: CPS1 results of scenario III for July 15

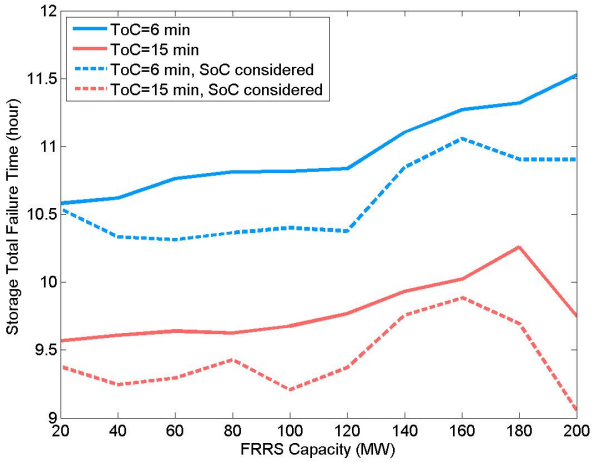

Figure 6.7: Storage failure time in scenario III for July 15

6.4.1.4 Results of Scenario III for October 23

Figure 6.8 and Figure 6.9 show the results of scenario III for October 23.

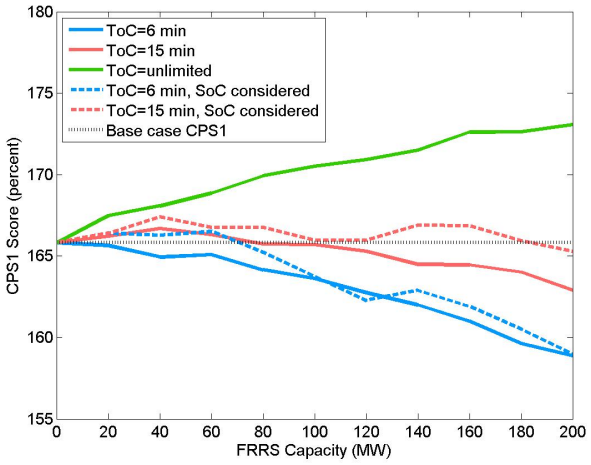

Figure 6.8: CPS1 results of scenario III for October 23

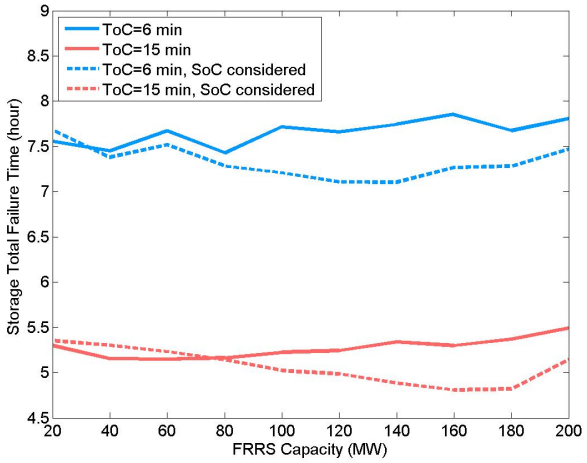

Figure 6.9: Storage failure time in scenario III for October 23

6.4.1.5 Discussion of Scenario III Results

Scenario III was tested for four selected days and the results were presented in Section 6.4.1.1 to Section 6.4.1.4 through two sets of figures. In the first set, each figure shows the CPS1 score of one selected day versus storage capacity providing FRRS in that day. This set includes Figure 6.2, Figure 6.4, Figure 6.6, and Figure 6.8. In the second set, each figure shows the total failure time of the FRRS provider during one selected day versus FRRS capacity. This set includes Figure 6.3, Figure 6.5, Figure 6.7, and Figure 6.9.

In both sets of figures, blue and red curves belong to the case of 6 minutes and 15 minutes ToC of the FRRS provider, respectively. Solid lines represent the results of original LFC methodology of scenario III and dashed lines represent modified logic, which considers SoC of the storage system.

It was expected that having longer ToC would result in less total failure time and consequently, better CPS1 compared to having shorter ToC. Comparing red and blue solid curves of both CPS1 and total failure time of all four days confirms these expectations. Similar conclusion can be drawn by comparing red and blue dashed curves, which are the results of modified logic.

In CPS1 plots, green curves show the results of employing scenario III while having a FRRS provider with unlimited energy storage capability. For all four days, green curves are above base case CPS1 scores, which are shown by dotted lines in CPS1 plots. For three days, the maximum improvement in CPS1 is about 3-4% of base case CPS1. Just in one day, the maximum

improvement is about 13%. These improvements show the effectiveness of using this scenario in an ideal condition of having unlimited stored energy.

Providing FRRS by a real energy storage system with limited stored energy will result in failures, which are expected to deteriorate CPS1 score compared to green curves. This hypothesis is also verified by the fact that in CPS1 plots of all days, red and blue curves are under the green curves. The adverse impacts of failures decreases CPS1 scores even below base case CPS1 for three days. In most cases, considering SoC (dashed curves) improves CPS1 compared to the original logic (solid curves). However, even with considering SoC, CPS1 is still less than base case CPS1.

One interesting observation is that in this scenario, variations in FRRS capacity do not make significant changes in total failure time of the storage system.

Overall, the outcomes of deploying ERCOT FRRS by the conventional regulation signal with proportional allocation method are not satisfactory. Even by having unlimited storage capability, this logic can not outstandingly improve ERCOT system frequency control performance. This is mostly due to the slow dynamic of the conventional regulation signal, which is not compatible with fast dynamic of the FRRS provider.

6.4.2 Scenario IV: Conventional Regulation Signal with Fast-First Allocation Method

In our fourth scenario, conventional regulation signal is used to deploy FRRS. However, FRRS is deployed and undeployed ahead of other resources. In this scenario, LFC determines total required regulation every 4 seconds. If additional regulation is required compared to the previous LFC cycle, first the storage resource will be asked to provide additional amount of regulation as much as its regulation responsibility allows. The rest will be requested from thermal generators proportionally to their responsibilities. The same procedure is in operation when regulation undeployment is required.

As an example of this scenario, Figure 6.10 shows deployment signals during first three hours of April 23 simulated by EFMAT. Conventional regulation signal is the total deployment signal for thermal generators and FRRS signal is deployment signal for an storage resource with FRRS responsibility of 40 MW. Figure 6.10 perfectly depicts the idea of deploying and undeploying FRRS ahead of conventional regulation whenever is required.

The LFC methodology of this scenario is tested by running EFMAT for four selected days. A storage resource with 6 minutes, 15 minutes, and unlimited ToC is assumed. In this scenario, LFC methodology can be modified to consider storage SoC in a way described in Section 6.4.1. Modified LFC methodology is also tested for each selected day assuming a storage resource with 6 minutes and 15 minutes ToC. CPS1 score of the whole day and the storage total failure time during the day is calculated for different FRRS ca-

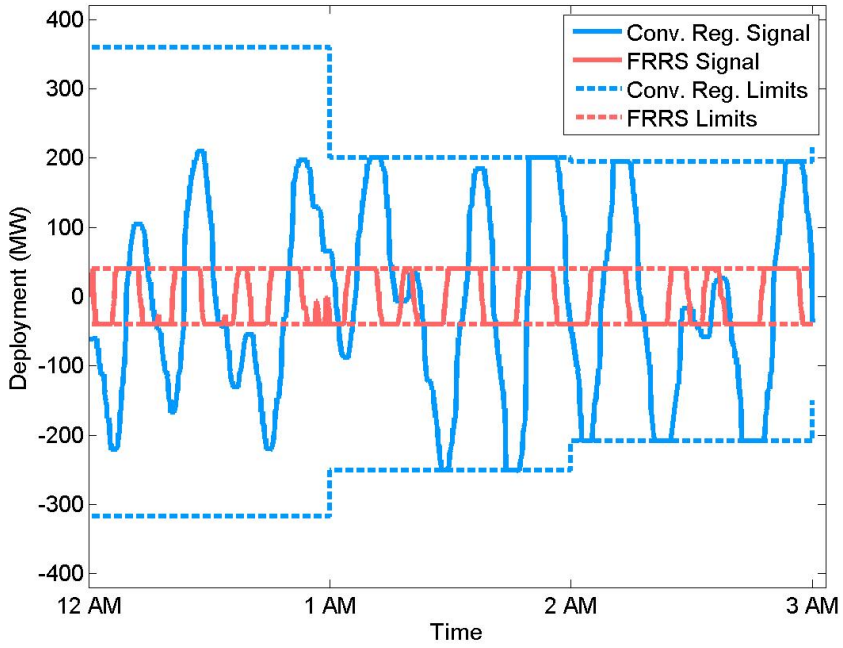

Figure 6.10: Deployment signals based on scenario IV during first three hours of April 23

pacities. The results will be presented and discussed in the following sections.

6.4.2.1 Results of Scenario IV for January 17

Figure 6.11 and Figure 6.12 show the results of scenario IV for January 17.

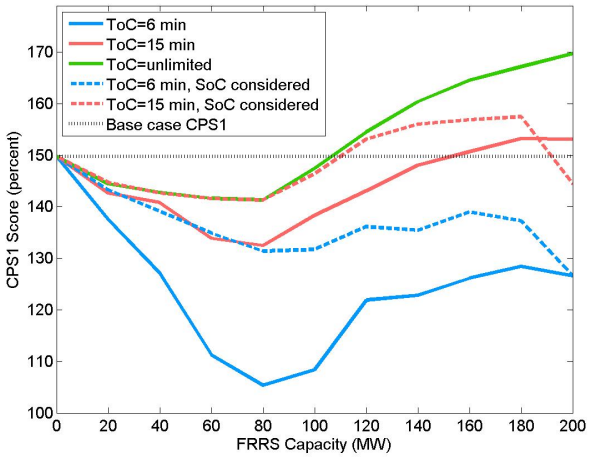

Figure 6.11: CPS1 results of scenario IV for January 17

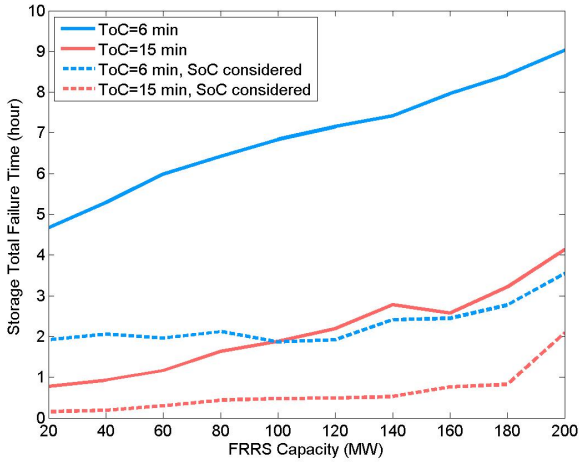

Figure 6.12: Storage failure time in scenario IV for January 17

6.4.2.2 Results of Scenario IV for April 23

Figure 6.13 and Figure 6.14 show the results of scenario IV for April 23.

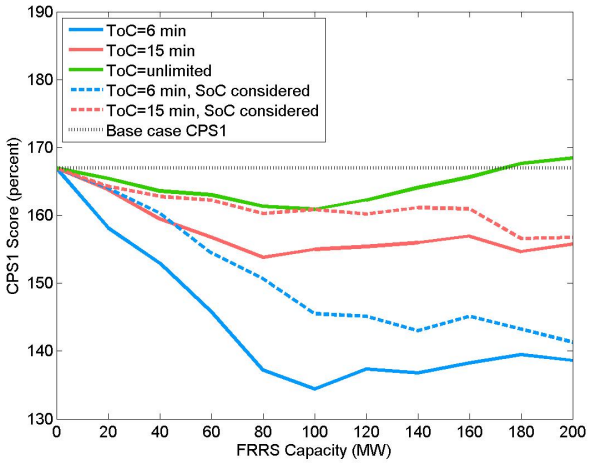

Figure 6.13: CPS1 results of scenario IV for April 23

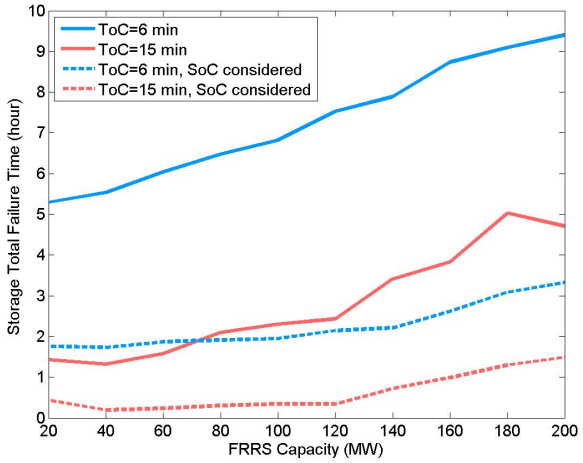

Figure 6.14: Storage failure time in scenario IV for April 23

6.4.2.3 Results of Scenario IV for July 15

Figure 6.15 and Figure 6.16 show the results of scenario IV for July 15.

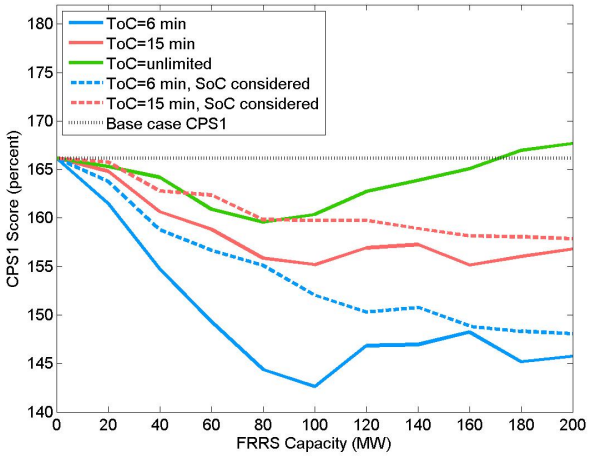

Figure 6.15: CPS1 results of scenario IV for July 15

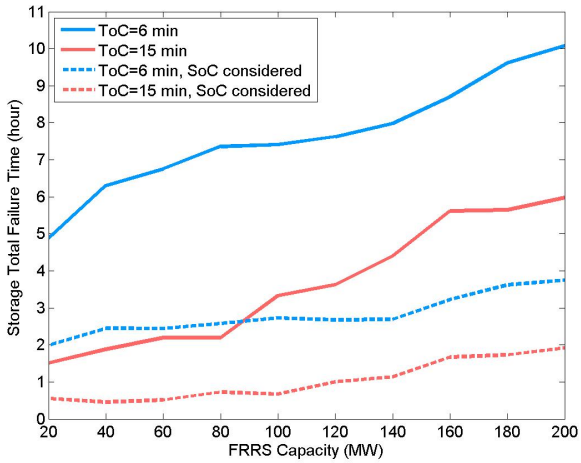

Figure 6.16: Storage failure time in scenario IV for July 15

6.4.2.4 Results of Scenario IV for October 23

Figure 6.17 and Figure 6.18 show the results of scenario IV for October 23.

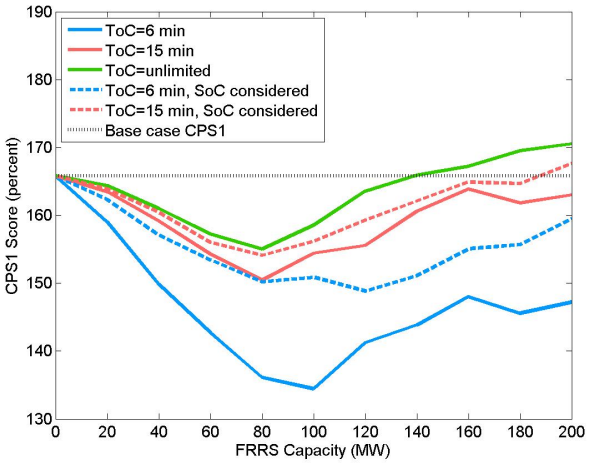

Figure 6.17: CPS1 results of scenario IV for October 23

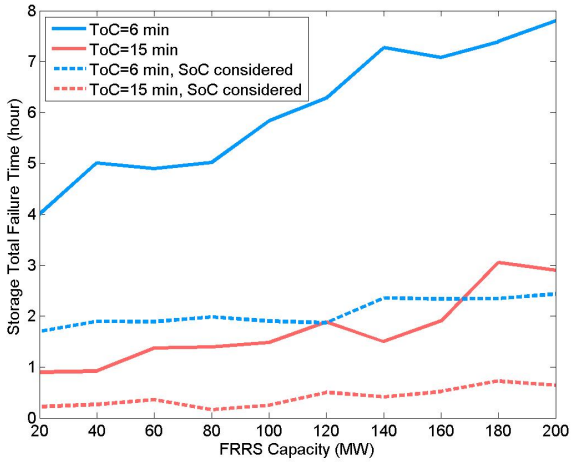

Figure 6.18: Storage failure time in scenario IV for October 23

6.4.2.5 Discussion of Scenario IV Results

Scenario IV was tested for four selected days and the results were presented in Section 6.4.2.1 to Section 6.4.2.4 through two sets of figures. In the first set, each figure shows the CPS1 score of one selected day versus storage capacity providing FRRS in that day. This set includes Figure 6.11, Figure 6.13, Figure 6.15, and Figure 6.17. In the second set, each figure shows the total failure time of the FRRS provider during one selected day versus FRRS capacity. This set includes Figure 6.12, Figure 6.14, Figure 6.16, and Figure 6.18.

Similar to the results of scenario III, in both sets of figures, blue and red curves belong to the case of 6 minutes and 15 minutes ToC of the FRRS provider, respectively. Solid lines represent the results of original LFC methodology of scenario IV and dashed lines represent modified logic, which considers SoC of the storage system.

Consistent with the expectations, having longer ToC results in less total failure time and consequently, better CPS1 compared to having shorter ToC in all cases of both original LFC methodology and the modified one.

In CPS1 plots, green curves show the results of employing scenario IV while having a FRRS provider with unlimited energy storage capability. For most cases, green curves are under base case CPS1 scores, which are shown by dotted lines in CPS1 plots. Just in some cases with higher FRRS capacity, CPS1 is improved compared to base case CPS1. For three days, the maximum

improvement in CPS1 is about 1-3% of base case CPS1. Just in one day, the improvement is about 13%.

Providing FRRS by energy storage systems with limited stored energy results in lower CPS1 scores of red and blue curves compared to green curves due to storage system failures. The adverse impacts of failures decrease CPS1 score even below base case CPS1 in almost all cases. In addition, in all cases, considering SoC (dashed curves) improves CPS1 compared to the original logic (solid curves) but CPS1 is still less than base case CPS1.

Contrary to the results of scenario III, in scenario IV changes in total failure time of the storage system due to the variations in FRRS capacity are not insignificant.

Overall, the outcomes of deploying FRRS by the conventional regulation signal with fast-first allocation method are not satisfactory. Even by having unlimited storage capability, this logic deteriorates system frequency control performance especially in cases with smaller FRRS capacities. This means that in this scenario, fast-responding regulation is not as effective as conventional regulation even by having a FRRS provider with unlimited energy storage capability. The situation becomes worse when the FRRS provider has limited energy storage capability.

6.5 Using Fast-Dynamic Signal to Deploy FRRS

As mentioned in Section 6.2, fast-responding regulation service is not deployed by conventional LFC signal in some power markets. Instead, a new signal with faster dynamic is derived from high oscillatory components of ACE. An example of this new signal is the PJM RegD signal. The LFC system of PJM calculates total required regulation by feeding ACE to a PI controller. The low frequency content of PI controller output determines RegA signal, which is the conventional regulation signal in PJM. RegD signal is derived from the difference of PI controller output and RegA signal[1]. This difference is in fact the high frequency content of PI controller output, which is slightly filtered by a low-pass filter to make RegD signal. PJM has also employed a mechanism to keep RegD signal neutral (i.e. centered around zero) over a short period of time in order to be more appropriate for energy limited resources. This mechanism attempts to make the signal neutral regardless of the impact on ACE control and also without considering the energy level of storage system [5, 33]. Based on PJM observations [32], when ACE deviation persists, RegD signal moves in the direction opposite to the desired control direction in order to keep its neutrality. This behavior negatively impacts system performance. Thus, recently PJM has proposed another mechanism called "conditional neutrality" [33]. In this mechanism, a controller constantly monitors storage SoC and sends feedback signals to RegA controller in order

[1]Personal communications with Danielle Croop, Sr. Engineer in the Performance Compliance department at PJM and also, Jason Sexauer, Engineer in the department of Outage Analysis Technologies at PJM

to help RegD providers keeping their SoC at 50% (i.e. half-charged). As the storage SoC becomes closer to its limits, larger feedback is calculated so that RegA can help bring the SoC back to 50% faster. This feedback is suspended whenever ACE deviation is larger than a threshold.

In the rest of this section, we will introduce scenarios V and VI in order to test ERCOT FRRS deployment by using a fast-dynamic signal. Then, optimal FRRS capacity and the equivalency ratio between FRRS and conventional regulation will be defined and calculated.

6.5.1 Scenario V: Fast-Dynamic Signal

In scenario V, conventional regulation is deployed by the traditional LFC signal. To deploy FRRS, LFC produces a new signal called fast-dynamic signal.

As described in Section 4.3.2, the ERCOT LFC system feeds ACE to a proportional controller with varying gain. The controller output will be processed by low-pass filters to determine required conventional regulation to be deployed. In this scenario, the difference between controller output and conventional regulation signal is the fast-dynamic signal used to deploy FRRS.

As an example of this scenario, Figure 6.19 shows deployment signals during first three hours of April 23 simulated by EFMAT. Conventional regulation signal is the total deployment signal for thermal generators and FRRS signal is fast-dynamic signal, which deploys an storage resource with FRRS responsibility of 40 MW. Comparing these two signals clarifies the concept of

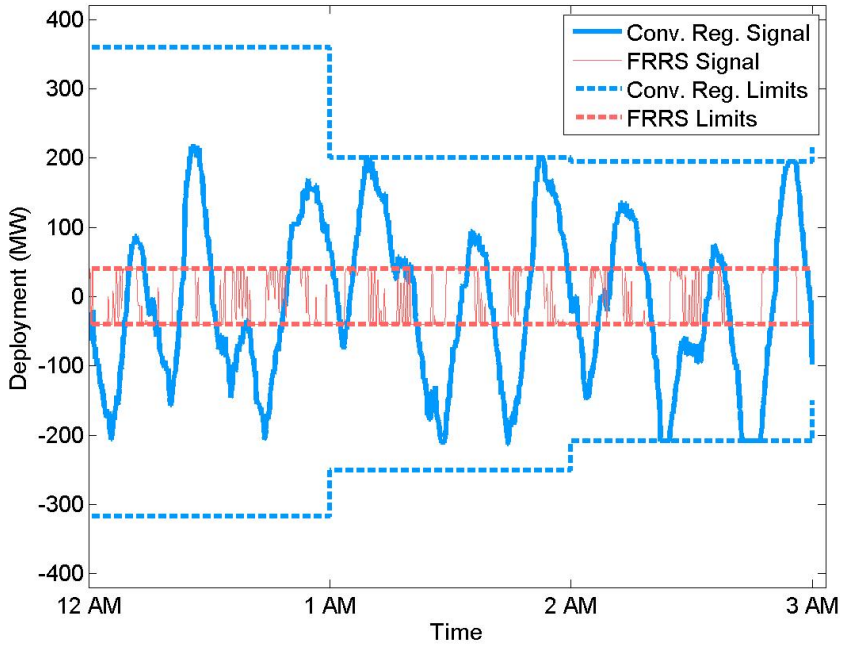

Figure 6.19: Deployment signals based on scenario V during first three hours of April 23

slow and fast dynamics.

In the original version of this scenario, whenever storage cannot respond to the signal due to being at maximum or minimum allowable level of stored energy, its output will become zero and storage will fail to provide the requested service.

To make RegD signal more appropriate for energy limited resources, PJM has proposed conditional neutrality mechanism described in previous section. The objective of this mechanism is to keep the storage SoC near midpoint by adjusting conventional regulation signal. We tested this mechanism

for the ERCOT system. The results showed that the mechanism negatively impacted CPS1. The resulting CPS1 scores were even below base case scores in some cases. Besides the results, we believe that it is not advantageous to get help from slow dynamics of RegA to restore storage SoC, which changes rapidly due to the fast cycling of storage system in response to RegD signal.

To make the fast-dynamic signal better-suited, we modified the signal to consider storage SoC. Another adjustment is also proposed in order to alleviate the adverse effects of storage failures. In the proposed version, if storage is unable to provide required FRRS due to its SoC level, deployment signal will move the current output of storage to zero level in three equal steps. This modification may push the storage SoC level beyond the limits. However, the duration of each step is calculated based on the ToC of the storage in a way that the worst resulted SoC will be out of limits by about one percent of maximum allowable limit. For example, the duration of each step is 4 seconds (i.e. one LFC cycle) for a storage with 6 minutes TOC and 8 seconds (i.e. two LFC cycles) for a storage with 15 minutes TOC.

This scenario is tested by running EFMAT for four selected days. A storage resource with 6 minutes, 15 minutes, and unlimited ToC is assumed. Also, modified signal that consider storage SoC is tested for each selected day assuming a storage resource with 6 minutes and 15 minutes ToC. CPS1 score of the whole day and the storage total failure time during the day is calculated for different FRRS capacities. The results will be presented and discussed in the following sections.

6.5.1.1 Results of Scenario V for January 17

Figure 6.20 and Figure 6.21 show the results of scenario V for January 17.

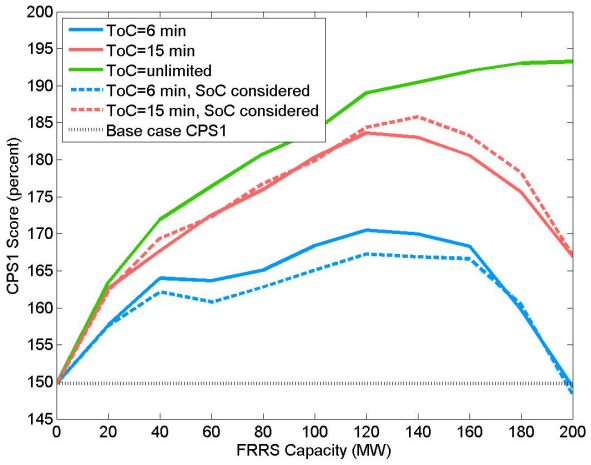

Figure 6.20: CPS1 results of scenario V for January 17

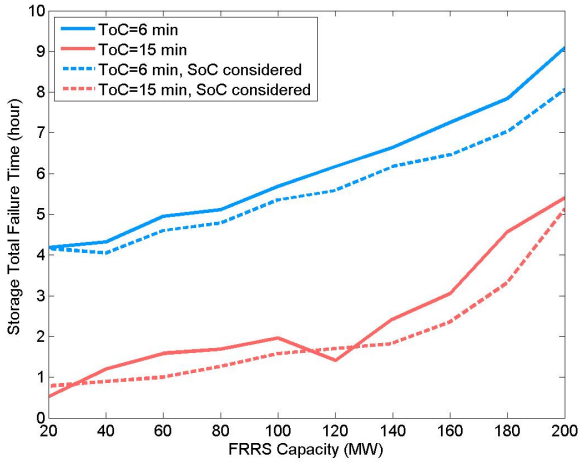

Figure 6.21: Storage failure time in scenario V for January 17

6.5.1.2 Results of Scenario V for April 23

Figure 6.22 and Figure 6.23 show the results of scenario V for April 23.

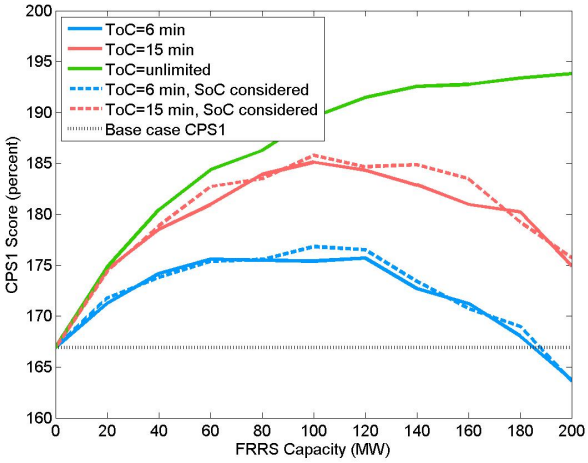

Figure 6.22: CPS1 results of scenario V for April 23

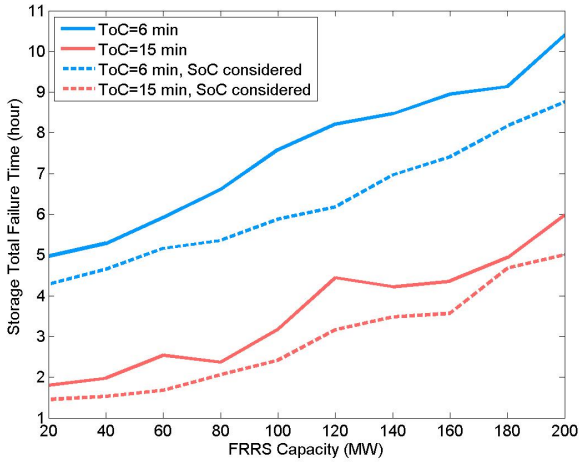

Figure 6.23: Storage failure time in scenario V for April 23

6.5.1.3 Results of Scenario V for July 15

Figure 6.24 and Figure 6.25 show the results of scenario V for July 15.

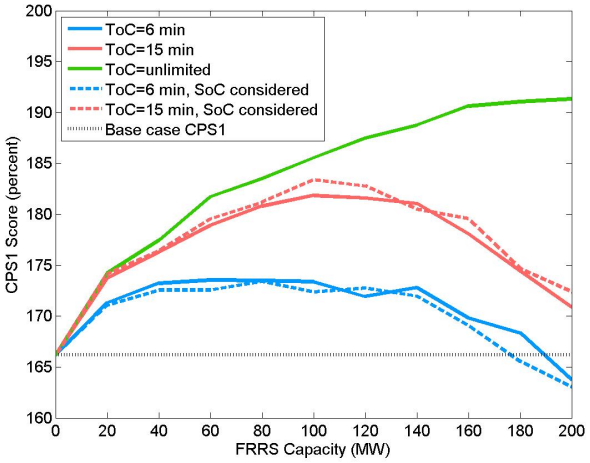

Figure 6.24: CPS1 results of scenario V for July 15

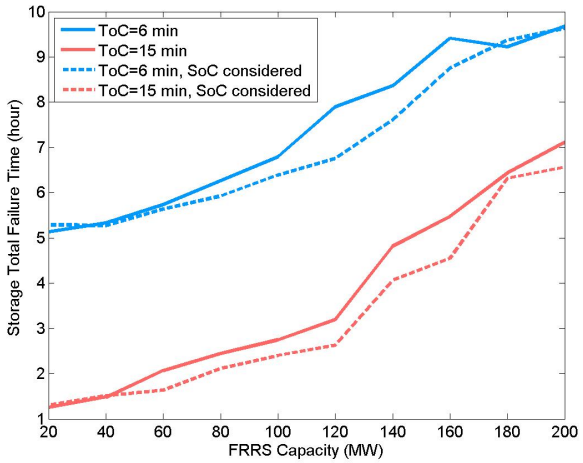

Figure 6.25: Storage failure time in scenario V for July 15

6.5.1.4 Results of Scenario V for October 23

Figure 6.26 and Figure 6.27 show the results of scenario V for October 23.

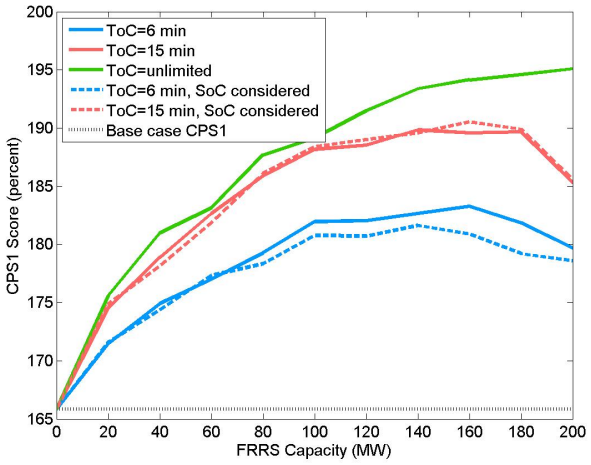

Figure 6.26: CPS1 results of scenario V for October 23

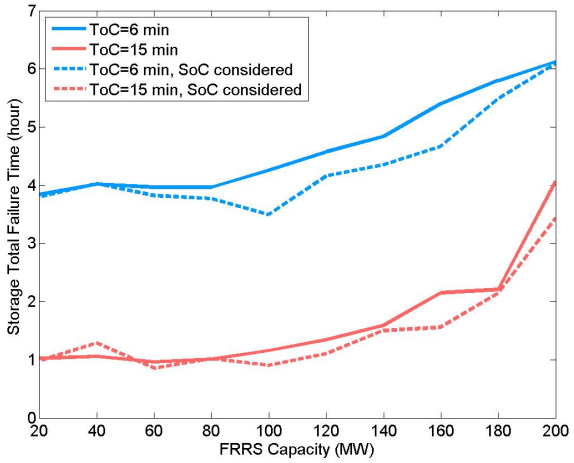

Figure 6.27: Storage failure time in scenario V for October 23

6.5.1.5 Discussion of Scenario V Results

Scenario V was tested for four selected days and the results were presented in Section 6.5.1.1 to Section 6.5.1.4 through two sets of figures. In the first set, each figure shows the CPS1 score of one selected day versus storage capacity providing FRRS in that day. This set includes Figure 6.20, Figure 6.22, Figure 6.24, and Figure 6.26. In the second set, each figure shows the total failure time of the FRRS provider during one selected day versus FRRS capacity. This set includes Figure 6.21, Figure 6.23, Figure 6.25, and Figure 6.27.

Similar to the results of previous scenarios, in both sets of figures, blue and red curves belong to the case of 6 minutes and 15 minutes ToC of the FRRS provider, respectively. Solid lines represent the results of original LFC methodology of scenario V and dashed lines represent modified logic, which considers SoC of the storage system.

Consistent with the expectations, having longer ToC results in less total failure time and consequently, better CPS1 compared to having shorter ToC in all cases of both original logic of this scenario and the modified one.

In CPS1 plots, green curves show the results of employing scenario V while having a FRRS provider with unlimited energy storage capability. For all cases, green curves are above base case CPS1 scores, which are shown by dotted lines in CPS1 plots. The maximum improvements in CPS1 in two of the four days are 15%, and in the other two days are 18% and 28% of base

case CPS1 scores. These improvements show the effectiveness of using this scenario in an ideal condition of having unlimited stored energy.

Providing FRRS by energy storage systems with limited stored energy results in lower CPS1 scores of red and blue curves compared to green curves due to storage system failures. However, CPS1 scores of red and blue curves are still above base case CPS1 in all cases with few exceptions. In addition, in almost all cases, considering SoC (dashed curves) decreased the storage failure time compared to the original logic (solid curves). Also, in some cases, considering SoC improved CPS1 compared to the original logic especially when the storage has 15 minutes ToC.

Overall, the performance of deploying FRRS by the fast-dynamic signal is significantly better than all previous scenarios. Even with a storage system having limited energy capability, CPS1 scores are improved compared to base cases for a wide range of FRRS capacities.

6.5.2 Scenario VI: Filtered Fast-Dynamic Signal

As mentioned before, PJM slightly filters the fast-dynamic signal and then uses it to deploy fast-responding resources. As CPS1 is calculated based on one-minute average of ACE, it may be concluded that responding to those ACE variations which are much faster than one minute is useless. Thus, fast-dynamic signal can be slightly filtered without lowering CPS1 and with the advantage of slower storage cycling. The purpose of scenario VI is to test this theory. In this scenario, fast-dynamic signal is filtered with a first-order

low-pass filter with 12 seconds time constant, which is considerably less than one minute.

This scenario is tested by running EFMAT for four selected days. A storage resource with 6 minutes, 15 minutes, and unlimited ToC is assumed. CPS1 score of the whole day and the storage total failure time during the day is calculated for different FRRS capacities. The results will be compared to the results of using unfiltered fast-dynamic signal. Both unfiltered and filtered signals are also adjusted to consider the storage SoC as proposed in scenario V in Section 6.5.1.

The results will be presented and discussed in the following sections.

6.5.2.1 Results of Scenario VI for January 17

Figure 6.28 and Figure 6.29 show the results of scenario VI for January 17.

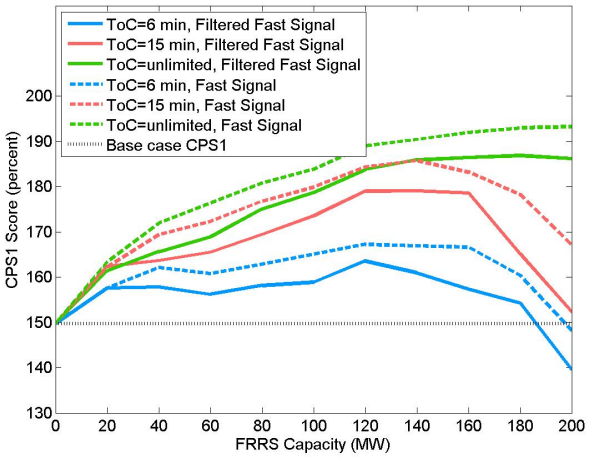

Figure 6.28: CPS1 results of scenario VI for January 17

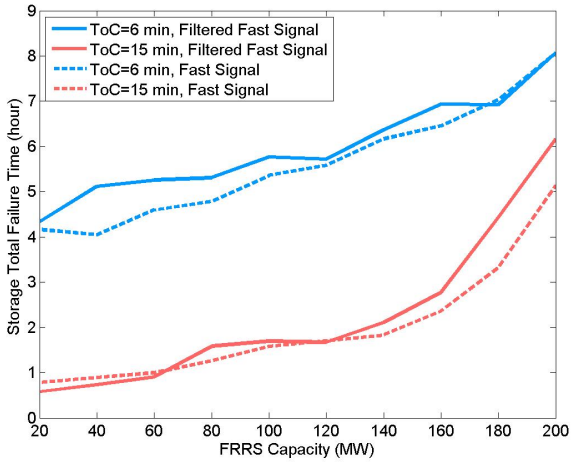

Figure 6.29: Storage failure time in scenario VI for January 17

6.5.2.2 Results of Scenario VI for April 23

Figure 6.30 and Figure 6.31 show the results of scenario VI for April 23.

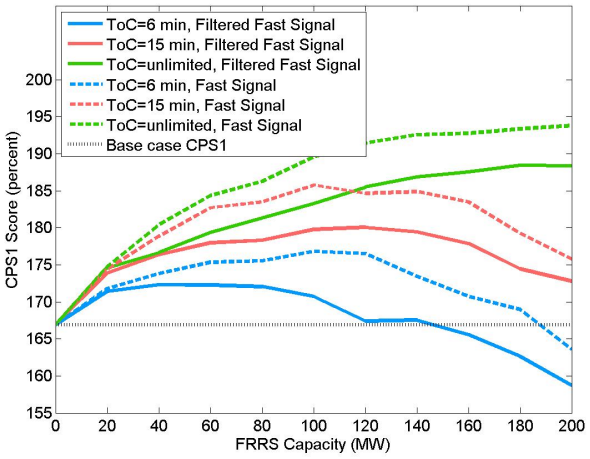

Figure 6.30: CPS1 results of scenario VI for April 23

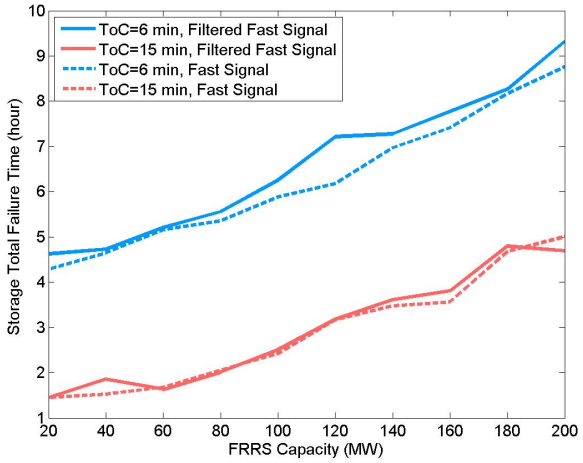

Figure 6.31: Storage failure time in scenario VI for April 23

6.5.2.3 Results of Scenario VI for July 15

Figure 6.32 and Figure 6.33 show the results of scenario VI for July 15.

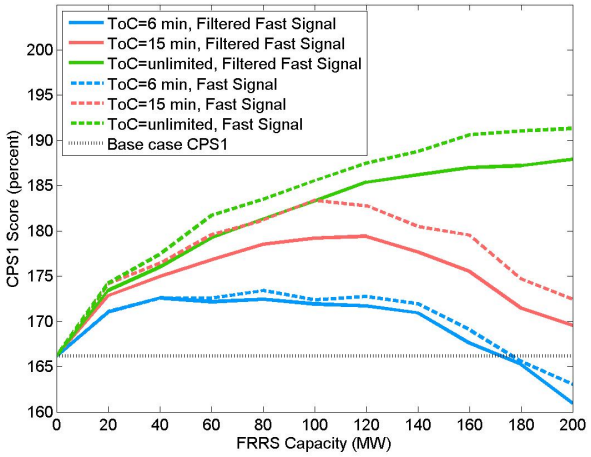

Figure 6.32: CPS1 results of scenario VI for July 15

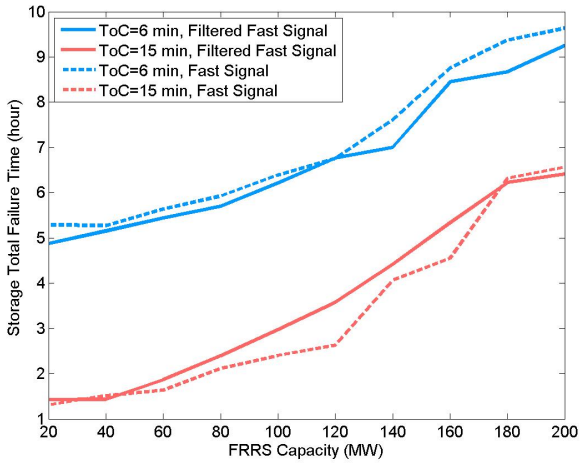

Figure 6.33: Storage failure time in scenario VI for July 15

6.5.2.4 Results of Scenario VI for October 23

Figure 6.34 and Figure 6.35 show the results of scenario VI for October 23.

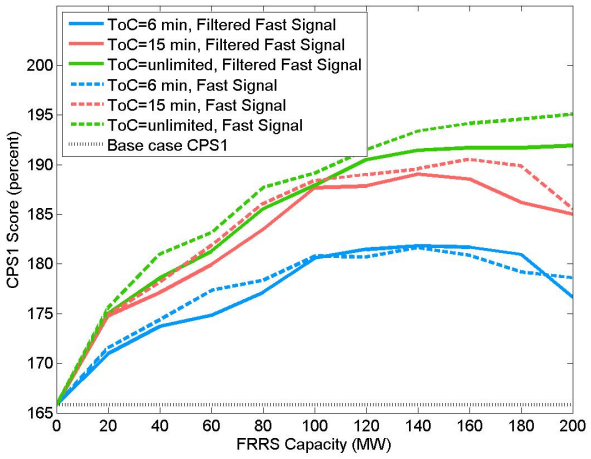

Figure 6.34: CPS1 results of scenario VI for October 23

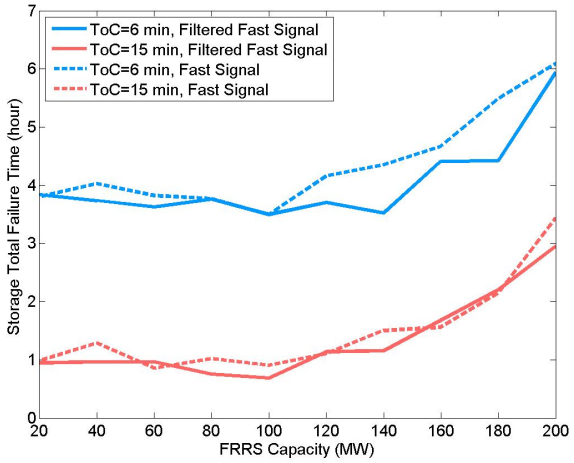

Figure 6.35: Storage failure time in scenario VI for October 23

6.5.2.5 Discussion of Scenario VI Results

Scenario VI was tested for four selected days and the results were presented in Section 6.5.2.1 to Section 6.5.2.4 through two sets of figures. In the first set, each figure shows the CPS1 score of one selected day versus storage capacity providing FRRS in that day. This set includes Figure 6.28, Figure 6.30, Figure 6.32, and Figure 6.34. In the second set, each figure shows the total failure time of the FRRS provider during one selected day versus FRRS capacity. This set includes Figure 6.29, Figure 6.31, Figure 6.33, and Figure 6.35.

Similar to the results of previous scenarios, in both sets of figures, blue, red, and green curves belong to the case of 6 minutes, 15 minutes, and unlimited ToC of the FRRS provider, respectively. Solid lines represent the results of using filtered fast-dynamic signal and dashed lines represent the results of using unfiltered fast-dynamic signal.

In all cases, filtering fast-dynamic signal leads to lower CPS1 scores compared to using unfiltered signal. In some cases with unlimited storage ToC, using filtered signal resulted in CPS1 scores even less than having 15 minutes storage ToC and using unfiltered signal. In addition, in most cases, using filtered signal causes larger total failure times compared to using unfiltered signal.

Based on the simulation results, filtering the fast-dynamic signal worsen CPS1 scores. The reason is that deploying FRRS by fast-dynamic signal has

two effects on ACE. One of these effects is to lower the amount of ACE deviations. The other effect is to increase the number of times ACE crosses zero. Both effects cause ACE to have smaller one-minute averages and hence, improve CPS1 compared to base case. When the signal is filtered, the number of ACE-zero crossings will be decreased, which will produce larger one-minute averages of ACE. Thus, resulting CPS1 scores using filtered signal will be less than CPS1 scores using unfiltered signal.

On the other hand, slower storage cycling resulted from using filtered signal may be beneficial to storage life time. However, slower cycling means deploying storage in one direction for longer periods of time and having less switchings between storage charging and discharging, which causes the storage SoC to reach the limits faster. That's why using filtered signal increases total failure time in some cases.

In summary, deploying FRRS by the filtered fast-dynamic signal is still beneficial to the system, however; the unfiltered signal can produce more improvement in system performance.

In the following section, optimal FRRS capacity and the equivalency ratio between FRRS and conventional regulation will be defined and calculated.

6.5.3 FRRS Optimal Capacity and Equivalency Ratio

Based on simulation results presented in previous sections, using the unfiltered fast-dynamic signal to deploy FRRS is the most advantageous method for ERCOT. Our proposed modifications to this method makes it more beneficial.

In order to investigate the effectiveness of using fast-responding resources to provide regulation service, two terms are defined in this section: FRRS optimal capacity and equivalency ratio.

As shown in CPS1 plots of scenario V, Figure 6.20, Figure 6.22, Figure 6.24, and Figure 6.26, there is a particular FRRS capacity (i.e. storage responsibility) for each studied day that results in largest improvement in CPS1 score compared to base case CPS1. This particular capacity is called optimal capacity in this dissertation.

For each of our base cases, total regulation requirement is procured from thermal generators. In other cases, total regulation requirements are shared between thermal generators and the storage system. In fact, in each of these cases, a portion of conventional regulation capacity is replaced by the same amount of FRRS capacity. In some cases, this replacement leads to an improvement in CPS1 score. This improvement means that the added FRRS capacity is more effective than the removed portion of conventional regulation capacity. By keeping the same FRRS capacity and gradually removing larger capacities of conventional regulation, CPS1 declines gradually till reach-

ing the base case CPS1. At this point, the FRRS capacity is as effective as the total removed conventional regulation capacity. The ratio between these two capacities is defined as equivalency ratio between FRRS and conventional regulation.

In this section, modified version of scenario V is tested for eight additional days from different months of 2014. The storage ToC is assumed 15 minutes. Figure 6.36 shows the CPS1 results of all eight days.

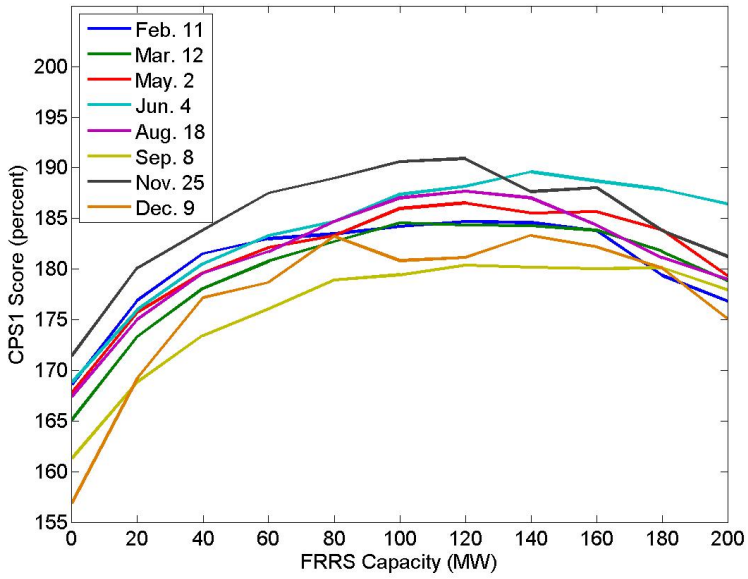

Figure 6.36: CPS1 results of scenario V with considering SoC for eight additional days - ToC is assumed 15 minutes.

The FRRS optimal capacity is determined for each of twelve historic days. Also, equivalency ratio is calculated for the FRRS optimal capacity of each day. Results listed in Table 6.1 show that the optimal capacity varies

from 100 MW to 160 MW and the equivalency ratio ranges from 1.6 up to 2.

Table 6.1: FRRS optimal capacity and equivalency ratio

Historic Day	Optimal Capacity	Equivalency Ratio
Jan. 17	140 MW	1.6
Feb. 11	120 MW	1.6
Mar. 12	100 MW	2
Apr. 23	140 MW	1.6
May 2	120 MW	1.8
Jun. 4	140 MW	1.8
Jul. 15	100 MW	1.7
Aug. 18	120 MW	1.8
Sep. 8	120 MW	1.8
Oct. 23	160 MW	1.6
Nov. 25	120 MW	1.9
Dec. 9	140 MW	1.6

In fact, the power of scenario V provides the opportunity to successfully integrate large capacities of fast-responding resources without lowering system performance. Our simulation results confirm that FRRS deployed by the proposed fast-dynamic signal can be up to two times more effective than conventional regulation.

Chapter 7

Conclusion

In recent years, fast-responding resources have participated in electricity markets and specifically frequency regulation markets. This dissertation investigated using these resources to provide fast-responding regulation service (FRRS) in ERCOT.

Simulating a power system to study frequency control needs a suitable model. In this dissertation, first we have proposed a simplified model of ERCOT frequency response. The main idea is to define dominant turbine types and substitute all units with the same type with a single unit modeled based on the dynamic behavior of its turbine type. Previous models usually have been constructed based on steam turbine technology. However, gas turbine is also one of the dominant generation types in ERCOT. Thus, an appropriately simplified model of a gas turbine has been included in the final model.

The final model of ERCOT frequency response is validated and tuned by using frequency measured by PMUs after 24 generation trip contingencies in ERCOT. Results show that despite nominal 5% governor droop settings of the majority of units, the model validation is not successful assuming 5% droop for equivalent turbines. In addition, values of tuned turbine time constants

cast doubt on using typical parameter values for equivalent turbine models as recommended and adopted in some studies. The tuned parameters can be used in model simulations to predict the system behavior for other circumstances. However, other conditions such as time of day or season may also affect the model parameter values which should be investigated in future studies.

This model represents the ERCOT system frequency response during a short period of time after a contingency. Hence, it is suitable for some particular studies especially the ones with the lack of information on system individual units. Considering the ultimate goal of this dissertation, a more comprehensive dynamic model representing system frequency behavior during normal conditions is required.

Thus, we developed a new tool called ERCOT Frequency Modeling and Analysis Tool (EFMAT), which is designed to simulate ERCOT system frequency and consists of three parts: pre-processing, Simulink model, and post-processing. The Simulink model includes all types of frequency control in the system and considers any other features of the system which may affect frequency. The tool is successfully verified and validated using actual frequency data.

Having a proper tool for our study, we run several simulations in order to evaluate the effectiveness of FRRS in ERCOT. Despite general impressions from most previous studies that fast regulation service is always beneficial, our preliminary results show that fast-responding resources can be helpful or harmful in controlling frequency. Also, the level of advantages or disadvantages

of fast-responding resources compared to conventional resources depends on how they are used and how much opportunity they have to be deployed.

Current ERCOT logic does not provide enough opportunity for fast-responding resources to help controlling frequency compared to the case just with conventional resources. Therefore, using FRRS even deteriorates CPS1 score. The first proposed adjustment to the logic was to narrow the trigger levels to be more compatible with narrower governors' deadbands. Updating the trigger levels to the proposed one resulted in better CPS1 compared to ERCOT trigger levels; however, CPS1 was still less than base case CPS1.

Another issue with ERCOT FRRS deployment logic is the prohibitively short deployment time. Consequently, energy limited logic was proposed which keeps track of produced or consumed energy instead of limiting the deployment time. Proposed energy limited logic combined with proposed trigger levels helps FRRS to be more beneficial for the system and improve CPS1 compared to base case. However, even this logic has some shortfalls.

Studying the policies of several other power systems across North America showed that most of them use ACE-derived signals to deploy fast-responding regulation.

The conventional regulation signal produced by LFC system has a slow dynamic, which makes it well-suited to deploy conventional regulation providers with slow ramping capabilities. However, the slow dynamic of this signal is not compatible with fast dynamic and also limited stored energy of

a storage system. Thus, using conventional signal to deploy fast-responding resources may not be an appropriate approach. The results of employing this approach in ERCOT showed that using conventional LFC signal to deploy FRRS will degrade system frequency control performance in most conditions.

Another approach is to produce a new ACE-derived signal having fast dynamics. Employing this approach in ERCOT resulted in significant improvements in the system performance. Considering storage SoC increased improvements in some cases. Simulation results of twelve historic days verified that using the fast-dynamic signal will enable participation of larger capacities of fast-responding resources without having adverse effects. Also, FRRS optimal capacity, which makes the largest improvement in CPS1, can be 1.6 to 2 times more effective than the same capacity of conventional regulation.

The work presented in this dissertation can be extended in multiple directions. First of all, EFMAT can be validated for historic days of 2016 when all governors had new settings. By having historic data and system settings during 2016, all simulations can also be repeated for selected historic days of 2016.

In our study, we assumed constant FRRS responsibility during a day. Also, FRRS UP responsibility was assumed equal to FRRS DN responsibility. In future studies, it will be useful to assume different FRRS UP and DN responsibilities for different hours of a day.

Another assumption in our work was to have a single storage sys-

tem providing FRRS. However, in reality, FRRS responsibility may be shared among several providers with different initial SoC and also different ToC. In the future, effectiveness of FRRS can be tested by assuming a combination of several providers with different characteristics.

Finally, we believe that our proposed modification to scenario V can be improved further in order to decrease storage failure time without degrading system performance.

Appendices

Appendix A

Function f_1 in the Gas Turbine Model

Before a contingency happens, the output of a gas turbine unit (P_0) is a function of both fuel signal (W) and the system frequency (f_0) [66]:

$$P_0 = [W f_0 + 0.5(1 - f_0)]\, f_0 \tag{A.1}$$

Before the contingency, the system frequency is near the nominal frequency. Therefore, it can be assumed that $1 - f_0 = 0$ and so:

$$P_0 = W f_0^2 \quad \Rightarrow \quad W = \frac{P_0}{{f_0}^2} \tag{A.2}$$

During first 10-15 seconds after the contingency, the fuel signal can be assumed constant; however, the frequency is changing rapidly and largely in this period of time. Therefore, the unit's output will change:

$$P(t) = [W f(t) + 0.5(1 - f(t))]\, f(t) \tag{A.3}$$

The change in unit's output ($\Delta P(t) = P(t) - P_0$) should be added to the change resulted from unit governor response. Function f_1 calculates this output change.

Function f_1:

$$\Delta P(t) = P_0[(\frac{f(t)}{f_0})^2 - 1] + 0.5f(t)(1 - f(t)) \tag{A.4}$$

Appendix B

ERCOT Methodologies for Determining Regulation Service Requirements

Based on ERCOT Nodal Protocol Section 3.16 [57], ERCOT must develop methodologies for determining the amounts of Ancillary Services requirements at least annually.

Here is the calculation method of base regulation requirements used prior to 2016 [58]:

"For determining the base Reg-Up requirements, ERCOT will take the largest of the 98.8 percentile of Reg-Up deployments over the last 30 days, the 98.8 percentile of Reg-Up deployments for the same month of the previous year, the 98.8 percentile of the positive Net Load changes over the last 30 days, and the 98.8 percentile of the positive Net Load changes for the same month of the previous year. For determining the base Reg-Down requirements, ERCOT will take the largest of the 98.8 percentile of Reg-Down deployments over the last 30 days, the 98.8 percentile of Reg-Down deployments for the same month of the previous year, the 98.8 percentile of the negative Net Load changes over the last 30 days, and the 98.8 percentile of the negative Net Load changes for the same month of the previous year."

From the beginning of 2016, this method is changed as below [58]:

"For determining the base Reg-Up requirements for a particular hour, ERCOT will take the largest of the 95th percentile of Reg-Up deployments for the same month of the previous two years, and the 95th percentile of the positive net load changes for the same month of the previous two years. For determining the base Reg-Down requirements, ERCOT will take the largest of the 95th percentile of Reg-Down deployments for the same month of the previous two years and the 95th percentile of the negative net load changes for the same month of the previous two years."

Bibliography

[1] Denis Lee Hau Aik. A general-order system frequency response model incorporating load shedding: analytic modeling and applications. *Power Systems, IEEE Transactions on*, 21(2):709–717, 2006. ISSN 0885-8950. doi:10.1109/TPWRS.2006.873123.

[2] P.M. Anderson and M. Mirheydar. A low-order system frequency response model. *Power Systems, IEEE Transactions on*, 5(3):720–729, 1990. ISSN 0885-8950. doi:10.1109/59.65898.

[3] P.M. Anderson and M. Mirheydar. An adaptive method for setting underfrequency load shedding relays. *Power Systems, IEEE Transactions on*, 7(2):647–655, 1992. ISSN 0885-8950. doi:10.1109/59.141770.

[4] A. Bagnasco, B. Delfino, G.B. Denegri, and S. Massucco. Management and dynamic performances of combined cycle power plants during parallel and islanding operation. *Energy Conversion, IEEE Transactions on*, 13 (2):194–201, June 1998. ISSN 0885-8969. doi:10.1109/60.678985.

[5] Scott Benner. A brief history of regulation signals at PJM, June 2015. URL `http://www.pjm.com/~/media/committees-groups/committees/oc/20150701-rpi/20150701-item-02-history-of-regulation-d.ashx`.

[6] Hassan Bevrani. *Robust power system frequency control*. Springer US, 2009.

[7] T. Borsche, A. Ulbig, M. Koller, and G. Andersson. Power and energy capacity requirements of storages providing frequency control reserves. In *2013 IEEE Power Energy Society General Meeting*, pages 1–5, July 2013. doi:10.1109/PESMG.2013.6672843.

[8] California ISO. Non-generator resource regulation energy management project implementation plan version 2.1, March 2012. URL `http://www.caiso.com/Documents/Non-GeneratorResourceRegulationEnergyManagementImplementationPlan.pdf`.

[9] D.S. Callaway and I.A. Hiskens. Achieving controllability of electric loads. *Proceedings of the IEEE*, 99(1):184–199, 2011. ISSN 0018-9219. doi:10.1109/JPROC.2010.2081652.

[10] Le Ren Chang-Chien, Luu Ngoc An, and Ta Wei Lin. Demand response plan considering available spinning reserve for system frequency restoration. In *Power System Technology (POWERCON), 2012 IEEE International Conference on*, pages 1–6, 2012. doi:10.1109/PowerCon.2012.6401353.

[11] G. Chavan, M. Weiss, A. Chakrabortty, S. Bhattacharya, A. Salazar, and F. Habibi-Ashrafi. Identification and predictive analysis of a

multi-area WECC power system model using synchrophasors. *IEEE Transactions on Smart Grid*, PP(99):1–1, 2016. ISSN 1949-3053. doi:10.1109/TSG.2016.2531637.

[12] J. Chen, P. Shrestha, S. H. Huang, N. D. R. Sarma, J. Adams, D. Obadina, and J. Ballance. Use of synchronized phasor measurements for dynamic stability monitoring and model validation in ERCOT. In *2012 IEEE Power and Energy Society General Meeting*, pages 1–7, July 2012. doi:10.1109/PESGM.2012.6345152.

[13] S. Chen, T. Zhang, H. B. Gooi, R. D. Masiello, and W. Katzenstein. Penetration rate and effectiveness studies of aggregated BESS for frequency regulation. *IEEE Transactions on Smart Grid*, 7(1):167–177, Jan 2016. ISSN 1949-3053. doi:10.1109/TSG.2015.2426017.

[14] Y. Chen, M. Keyser, M. H. Tackett, and X. Ma. Incorporating short-term stored energy resource into Midwest ISO energy and ancillary service market. *IEEE Transactions on Power Systems*, 26(2):829–838, May 2011. ISSN 0885-8950. doi:10.1109/TPWRS.2010.2061875.

[15] J. Cleary, M. L. Lazarewicz, L. Nelson, R. Rounds, and J. Arsenault. Interconnection study: 5MW of Beacon Power flywheels on 23 kV line, Tyngsboro, MA. In *Innovative Technologies for an Efficient and Reliable Electricity Supply (CITRES), 2010 IEEE Conference on*, pages 285–291, Sept 2010. doi:10.1109/CITRES.2010.5619793.

[16] Federal Energy Regulatory Commission. Preventing undue discrimination and preference in transmission service. FERC Order NO. 890, February 2007. URL http://www.ferc.gov/whats-new/comm-meet/2007/021507/E-1.pdf.

[17] Federal Energy Regulatory Commission. Frequency regulation compensation in the organized wholesale power markets. FERC Order NO. 755, October 2011. URL http://www.ferc.gov/whats-new/comm-meet/2011/102011/E-28.pdf.

[18] North American Electric Reliability Corporation. Waiver Request - Control Performance Standard 2, November 2002. URL http://www.nerc.com/files/Waivers.pdf.

[19] North American Electric Reliability Corporation. Standard BAL-001-0.1a: Real power balancing control performance, May 2009. URL http://www.nerc.com/files/BAL-001-0_1a.pdf.

[20] North American Electric Reliability Corporation. Balancing and frequency control, January 2011. URL http://www.nerc.com/docs/oc/rs/NERC%20Balancing%20and%20Frequency%20Control%20040520111.pdf.

[21] G. Delille, B. Francois, and G. Malarange. Dynamic frequency control support: A virtual inertia provided by distributed energy storage to isolated power systems. In *Innovative Smart Grid Technologies*

Conference Europe (ISGT Europe), 2010 IEEE PES, pages 1–8, 2010. doi:10.1109/ISGTEUROPE.2010.5638887.

[22] P. Du and Y. Makarov. Using disturbance data to monitor primary frequency response for power system interconnections. *IEEE Transactions on Power Systems*, 29(3):1431–1432, May 2014. ISSN 0885-8950. doi:10.1109/TPWRS.2013.2288013.

[23] POTOMAC ECONOMICS. 2014 state of the market report for the ERCOT wholesale electricity markets, July 2015. URL `https://www.potomaceconomics.com/uploads/ercot_documents/2014_ERCOT_State_of_the_Market_Report.pdf`.

[24] Texas Reliability Entity. Standard BAL-001-TRE-1: Primary frequency response in the ERCOT region, January 2014. URL `http://www.nerc.com/pa/Stand/Reliability%20Standards/BAL-001-TRE-1.pdf`.

[25] J.H. Eto et al. Use of frequency response metrics to assess the planning and operating requirements for reliable integration of variable renewable generation, December 2010. URL `http://www.ferc.gov/industries/electric/indus-act/reliability/frequencyresponsemetrics-report.pdf`.

[26] D. Fooladivanda, C. Rosenberg, and S. Garg. An analysis of energy storage and regulation. In *Smart Grid Communications (SmartGridComm), 2014 IEEE International Conference on*, pages 91–96, Nov 2014. doi:10.1109/SmartGridComm.2014.7007628.

[27] D. Fooladivanda, C. Rosenberg, and S. Garg. Energy storage and regulation: An analysis. *IEEE Transactions on Smart Grid*, 7(4):1813–1823, July 2016. ISSN 1949-3053. doi:10.1109/TSG.2015.2494841.

[28] A. A. Hajnoroozi, F. Aminifar, and H. Ayoubzadeh. Generating unit model validation and calibration through synchrophasor measurements. *IEEE Transactions on Smart Grid*, 6(1):441–449, Jan 2015. ISSN 1949-3053. doi:10.1109/TSG.2014.2322821.

[29] J. F. Hauer, W. A. Mittelstadt, K. E. Martin, J. W. Burns, H. Lee, J. W. Pierre, and D. J. Trudnowski. Use of the WECC WAMS in wide-area probing tests for validation of system performance and modeling. *IEEE Transactions on Power Systems*, 24(1):250–257, Feb 2009. ISSN 0885-8950. doi:10.1109/TPWRS.2008.2009429.

[30] Z. Huang, P. Du, D. Kosterev, and S. Yang. Generator dynamic model validation and parameter calibration using phasor measurements at the point of connection. *IEEE Transactions on Power Systems*, 28(2):1939–1949, May 2013. ISSN 0885-8950. doi:10.1109/TPWRS.2013.2251482.

[31] T. Inoue, H. Taniguchi, and Y. Ikeguchi. A model of fossil fueled plant with once-through boiler for power system frequency simulation studies. *Power Systems, IEEE Transactions on*, 15(4):1322–1328, 2000. ISSN 0885-8950. doi:10.1109/59.898108.

[32] PJM Interconnection. Fast response regulation (RegD) resources operational impact, 2015. URL `http://www.pjm.com/`

~/media/committees-groups/committees/oc/20150526-rpi/20150526-item-02-problem-statement.ashx.

[33] PJM Interconnection. Conditional Neutrality, 2016. URL http://www.pjm.com/~/media/committees-groups/task-forces/rmistf/20160830/20160830-item-03-conditional-neutrality.ashx.

[34] ISO New England. Description of the Energy Neutral AGC dispatch algorithm, March 2015. URL http://www.iso-ne.com/static-assets/documents/2015/03/energy_neutral_dispatch_algorithms.pdf.

[35] N. Jaleeli and L.S. Vanslyck. NERC's new control performance standards. *Power Systems, IEEE Transactions on*, 14(3):1092–1099, August 1999. ISSN 0885-8950. doi:10.1109/59.780932.

[36] C. Jin, N. Lu, S. Lu, Y. V. Makarov, and R. A. Dougal. A coordinating algorithm for dispatching regulation services between slow and fast power regulating resources. *IEEE Transactions on Smart Grid*, 5(2):1043–1050, March 2014. ISSN 1949-3053. doi:10.1109/TSG.2013.2277974.

[37] Y. J. Kim, G. Del-Rosario-Calaf, and L. K. Norford. Analysis and experimental implementation of grid frequency regulation using behind-the-meter batteries compensating for fast load demand variations. *IEEE Transactions on Power Systems*, PP(99):1–1, 2016. ISSN 0885-8950. doi:10.1109/TPWRS.2016.2561258.

[38] B. Kirby. Ancillary services: Technical and commercial insights, 2007. URL http://consultkirby.com/files/Ancillary_Services_-_Technical_And_Commercial_Insights_EXT_.pdf.

[39] D. Kosterev. Hydro turbine-governor model validation in Pacific Northwest. *IEEE Transactions on Power Systems*, 19(2):1144–1149, May 2004. ISSN 0885-8950. doi:10.1109/TPWRS.2003.821464.

[40] Prabha Kundur. *Power system stability and control*. McGraw-Hill, Inc., 1994.

[41] G. Lalor. *Frequency Control on an Island Power System with Evolving Plant Mix*. PhD thesis, University College Dublin, 2005. URL http://erc.ucd.ie/files/theses/Gill%20Lalor%20-%20Frequency%20Control%20on%20an%20Island%20Power%20System%20with%20Evolving%20Plant%20Mix.pdf.

[42] G. Lalor, J. Ritchie, D. Flynn, and M.J. O'Malley. The impact of combined-cycle gas turbine short-term dynamics on frequency control. *Power Systems, IEEE Transactions on*, 20(3):1456–1464, August 2005. ISSN 0885-8950. doi:10.1109/TPWRS.2005.852058.

[43] M. L. Lazarewicz and A. Rojas. Grid frequency regulation by recycling electrical energy in flywheels. In *Power Engineering Society General Meeting, 2004. IEEE*, pages 2038–2042 Vol.2, June 2004. doi:10.1109/PES.2004.1373235.

[44] M. L. Lazarewicz and T. M. Ryan. Integration of flywheel-based energy storage for frequency regulation in deregulated markets. In *IEEE PES General Meeting*, pages 1–6, July 2010. doi:10.1109/PES.2010.5589748.

[45] Wanning Li and Y. Chen. MISO AGC enhancement proposal to better utilize fast ramping resources. In *2015 IEEE Power Energy Society General Meeting*, pages 1–5, July 2015. doi:10.1109/PESGM.2015.7285889.

[46] J. Lin, G. Damato, and P. Hand. Energy storage: A cheaper, faster, and cleaner alternative to conventional frequency regulation. Prepared for the California Energy Storage Alliance, February 2011. URL `http://www.iceenergy.com/stuff/contentmgr/files/1/76d44bfc1077e7fad6425102e55c0491/download/cesa_energy_storage_for_frequency_regulation.pdf`.

[47] Jan Machowski, Janusz Bialek, and Jim Bumby. *Power system dynamics: stability and control*. Wiley, 2011.

[48] P. Mackin et al. Dynamic simulation studies of the frequency response of the three U.S. interconnections with increased wind generation, December 2010. URL `http://www.ferc.gov/industries/electric/indus-act/reliability/frequencyresponsemetrics-report.pdf`.

[49] Y. Makarov et al. Assessing the value of regulation resources based on their time response characteristics. Prepared by Pacific Northwest National Laboratory for the California Energy Commission, June 2008. URL `http://certs.lbl.gov/pdf/task-2-4-regulation-resources.pdf`.

[50] R. Masiello et al. Research evaluation of wind generation, solar generation, and storage impact on the California grid. Prepared by KEMA Inc. for the California Energy Commission, Public Interest Energy Research Program, June 2010. URL http://www.energy.ca.gov/2010publications/CEC-500-2010-010/CEC-500-2010-010.PDF.

[51] P. Mercier, R. Cherkaoui, and A. Oudalov. Optimizing a battery energy storage system for frequency control application in an isolated power system. *IEEE Transactions on Power Systems*, 24(3):1469–1477, Aug 2009. ISSN 0885-8950. doi:10.1109/TPWRS.2009.2022997.

[52] S. Mirzazad-Barijough, M. Mashhuri, and A.M. Ranjbar. A predictive approach to control frequency instabilities in a wide area system. In *Power Systems Conference and Exposition, 2009. PSCE '09. IEEE/PES*, pages 1–6, 2009. doi:10.1109/PSCE.2009.4840142.

[53] New York ISO. Energy storage in the new york electricity markets, March 2010. URL http://www.nyiso.com/public/webdocs/media_room/publications_presentations/White_Papers/White_Papers/Energy_Storage_in_the_NY_Electricity_Market_March2010.pdf.

[54] Electric Reliability Council of Texas. ERCOT comments to NPRR 377: Alternate inputs to base point deviation charge, September 2011. URL http://www.ercot.com/content/mktrules/issues/nprr/376-400/377/keydocs/377NPRR-12_ERCOT_Comments_092111.doc.

[55] Electric Reliability Council of Texas. ERCOT Fast-Responding Regulation Service. webpage for FRRS Pilot Project, 2012. URL http://www.ercot.com/mktrules/pilots/frrs.

[56] Electric Reliability Council of Texas. ERCOT Nodal Operating Guides, Section 2: System operations and control requirements, December 2014. URL http://www.ercot.com/content/mktrules/guides/noperating/2014/12/December_1,_2014_Nodal_Operating_Guides.pdf.

[57] Electric Reliability Council of Texas. ERCOT Nodal Protocols, Section 3: Management activities for the ercot system, September 2016. URL http://www.ercot.com/content/wcm/current_guides/53528/03_090116_Nodal.doc.

[58] Electric Reliability Council of Texas. ERCOT methodologies for determining ancillary service requirements, 2016. URL http://www.ercot.com/content/wcm/key_documents_lists/89135/ERCOT_Methodologies_for_Determining_Ancillary_Service_Requirements.zip.

[59] Electric Reliability Council of Texas. Governing document for Fast-Responding Regulation Service pilot project, July, 2013. URL http://www.ercot.com/content/mktrules/pilots/frrs/FRRS_Governing_Document_(July_Board)_7_17_13_Amended_Blackli.doc.

[60] Electric Reliability Council of Texas. ERCOT Quick Facts, September,

2016. URL http://www.ercot.com/content/wcm/lists/89475/ERCOT_Quick_Facts_9916.pdf.

[61] Electric Reliability Council of Texas. About ERCOT, September, 2016. URL http://www.ercot.com/about/.

[62] P. Overholt, D. Kosterev, J. Eto, S. Yang, and B. Lesieutre. Improving reliability through better models: Using synchrophasor data to validate power plant models. *IEEE Power and Energy Magazine*, 12(3):44–51, May 2014. ISSN 1540-7977. doi:10.1109/MPE.2014.2301533.

[63] X. Pan, H. Xu, J. Song, and C. Lu. Capacity optimization of battery energy storage systems for frequency regulation. In *2015 IEEE International Conference on Automation Science and Engineering (CASE)*, pages 1139–1144, Aug 2015. doi:10.1109/CoASE.2015.7294251.

[64] Hongyan Piao, Shifeng Chen, Haichao Lv, and Haoming Liu. Control strategy of battery energy storage system to participate in the second frequency regulation. In *Smart Electric Distribution Systems and Technologies (EDST), 2015 International Symposium on*, pages 53–57, Sept 2015. doi:10.1109/SEDST.2015.7315182.

[65] I. C. Report. Dynamic models for steam and hydro turbines in power system studies. *IEEE Transactions on Power Apparatus and Systems*, PAS-92(6):1904–1915, Nov 1973. ISSN 0018-9510. doi:10.1109/TPAS.1973.293570.

[66] William I Rowen. Simplified mathematical representations of heavy-duty gas turbines. *ASME Journal of Engineering for Power*, 105(4):865–869, 1983.

[67] William I Rowen. Simplified mathematical representations of single shaft gas turbines in mechanical drive service. *Turbomacjnary International*, pages 26–32, July/August 1992.

[68] U. Rudez and R. Mihalic. Analysis of underfrequency load shedding using a frequency gradient. *Power Delivery, IEEE Transactions on*, 26(2):565–575, 2011. ISSN 0885-8977. doi:10.1109/TPWRD.2009.2036356.

[69] S. Sharma, Huang Shun-Hsien, and N. D R Sarma. System inertial frequency response estimation and impact of renewable resources in ERCOT interconnection. In *Power and Energy Society General Meeting, 2011 IEEE*, pages 1–6, July 2011. doi:10.1109/PES.2011.6038993.

[70] M. R B Tavakoli, B. Vahidi, and W. Gawlik. An educational guide to extract the parameters of heavy duty gas turbines model in dynamic studies based on operational data. *Power Systems, IEEE Transactions on*, 24(3):1366–1374, August 2009. ISSN 0885-8950. doi:10.1109/TPWRS.2009.2021231.

[71] V.V. Terzija. Adaptive underfrequency load shedding based on the magnitude of the disturbance estimation. *Power Systems, IEEE Transactions on*, 21(3):1260–1266, 2006. ISSN 0885-8950. doi:10.1109/TPWRS.2006.879315.

[72] D. Tyagi, A. Kumar, and S. Chanana. Load shedding via PID controller for an isolated power system. In *Power India Conference, 2012 IEEE Fifth*, pages 1–6, 2012. doi:10.1109/PowerI.2012.6479461.

[73] Khoi Vu, R. Masiello, and R. Fioravanti. Benefits of fast-response storage devices for system regulation in ISO markets. In *Power Energy Society General Meeting, 2009. PES '09. IEEE*, pages 1–8, July 2009. doi:10.1109/PES.2009.5275922.

[74] B. Xu, Y. Dvorkin, and D. S. Kirschen. A comparison of policies on the participation of storage in U.S. frequency regulation markets, February 2016. URL `https://arxiv.org/pdf/1602.04420.pdf`.

[75] Soon Kiat Yee, J.V. Milanovic, and F.M. Hughes. Overview and comparative analysis of gas turbine models for system stability studies. *Power Systems, IEEE Transactions on*, 23(1):108–118, February 2008. ISSN 0885-8950. doi:10.1109/TPWRS.2007.907384.

[76] F. Zhang, M. Tokombayev, Y. Song, and G. Gross. Effective flywheel energy storage (FES) offer strategies for frequency regulation service provision. In *Power Systems Computation Conference (PSCC), 2014*, pages 1–7, Aug 2014. doi:10.1109/PSCC.2014.7038427.

[77] Q. Zhang and P.L. So. Dynamic modelling of a combined cycle plant for power system stability studies. In *Power Engineering Society Winter Meeting, 2000. IEEE*, volume 2, pages 1538–1543 vol.2, 2000. doi:10.1109/PESW.2000.850211.

[78] M. Zima, M. Larsson, P. Korba, C. Rehtanz, and G. Andersson. Design aspects for wide-area monitoring and control systems. *Proceedings of the IEEE*, 93(5):980–996, 2005. ISSN 0018-9219. doi:10.1109/JPROC.2005.846336.

Vita

Mansoureh Peydayesh received her BSc Degree in Electrical Engineering from Sharif University of Technology, Iran in 2006. In the same year, she joined the graduate program of the University of Tehran and earned her MSc in Electrical Engineering in 2008. She pursued her studies joining the graduate program at the University of Texas at Austin in 2009. Working on frequency control in power system under supervision of Professor Ross Baldick, she finished her PhD in 2016. She also served as a research intern at the Electric Reliability Council of Texas (ERCOT) form June 2015 to May 2016.

Email address: mpeydayesh@utexas.edu,
peydayesh.m@gmail.com

This dissertation was typeset with LaTeX[†] by the author.

[†]LaTeX is a document preparation system developed by Leslie Lamport as a special version of Donald Knuth's TeX Program.